UBV PHOTOMETRY OF MARS

A. T. YOUNG

*Jet Propulsion Laboratory, California Institute of Technology, Pasadena, Calif., U.S.A.**

Abstract. A critical analysis of selected high-quality photometric observations of Mars indicates that: (1) The phase function is concave upward out to at least 40° phase. No *sudden* brightening occurs at opposition, but the curvature increases at small phase. (2) Large systematic differences (0.1–0.2 mag.) exist between different observers' data. However, the small random scatter attributable to Mars (0.01–0.02 mag.) in the better series suggests that these differences represent systematic errors in data reduction, not variations in the planet's brightness. (3) The disentangling of seasonal, diurnal, and phase effects leaves considerable ambiguity; more observations are needed, over a long time, with a stable instrumental system. However, even the present data are sufficient to expose substantial errors in published phase curves of Mars (and consequently, in interpretations based on them).

1. Introduction

Ground-based photometry of Mars is primarily useful for determining the phase function of the planet. It can also be used to study large-scale atmospheric and surface changes, such as 'blue clearings' and seasonal variations.

Accurate photoelectric observations of Mars were first made by Guthrick and Prager (1914), who discovered the rotational effect, with maximum brightness near longitude 100°. Unfortunately it is not possible to reduce their data to any modern photometric system. The first UBV observations were made by Johnson and Gardiner (1955), who misinterpreted their data owing to an error in computing central meridians. In re-analyzing their data, I suggested 'a real brightening of Mars by one- or two-tenths of a magnitude at phase angles less than about 12°' (Young, 1957). This suggestion was repeated by de Vaucouleurs (1960), who made additional observations in 1958; however, his data (which cover only 3 nights) were too limited to establish the effect with certainty. I therefore made additional observations, especially at small phase angles, during the 1960–61 opposition. Even from these data I was unable to reach a definite conclusion, so I resolved to postpone a full discussion until the completion of the extensive Harvard-NASA program of planetary photometry (Young and Irvine, 1967). These data are now available (Irvine *et al.*, 1968a, b) and, although a definitive solution still is not possible, the problem is clear enough to permit a preliminary discussion.

It must be admitted at once that the UBV system is poorly suited to Martian photometry. The V band is situated in the steepest part of the Martian reflectance spectrum, so that slight errors in reducing 'V' data to a common system produce considerable systematic errors in the results. The V band is also poorly placed to display the rotational effect (Irvine *et al.*, 1968), which is stronger at longer wavelengths. Furthermore, Mars is so red ($B-V \approx +1.4$) that red-leak corrections (Shao and Young, 1965) are important in the ultraviolet; if corrections are merely estimated from the colors, systematic errors due to the peculiar spectral energy distribution of the planet can be

* Present address: Dept. of Physics, Texas A. and M. University, College Station, Tex. 77843, U.S.A.

Woszczyk and Iwaniszewska (eds.), Exploration of the Planetary System, 253–285.

expected. On the other hand, the UBV data are the only ones with enough time span to allow one to look for (Martian) seasonal effects, as several different oppositions have been observed.

2. Photometric Central Meridian

Previous investigators have analyzed the rotational light curve in terms of the areographic longitude of the center of the disc, which is tabulated for 0^h UT of each day in the Astronomical Ephemeris. However, the phase of Mars near quadrature is so large that the center of the disc is not suitable as a reference meridian for photometry, since an appreciable portion of the terminator side of the disc is in shadow. We need to define a *photometric* central meridian.

It is easy to show that the effective photometric center of the disc lies halfway between the subsolar point and the center of the disc. For, consider a photometric longitude l measured from this 'mirror' meridian, which is perpendicular to the photometric equator (the great circle through the subsolar point and the center of the disc); at phase angle α, the photometric longitude runs from $(90° - \alpha/2)$ at the limb to $-(90° - \alpha/2)$ at the terminator. We want to find the mean longitude, weighting each element of area dA on the planet by its apparent projected area and surface brightness. If i and ε are the angles of incidence and emission, measured from the local normal, the projected area is $\cos\varepsilon\, dA$.

Now consider two similar elements of area $dA = dA'$ related by the reciprocity principle (Minnaert, 1962), so that $i' = \varepsilon$ and $\varepsilon' = i$; they are symmetrically placed about $l = 0$, so that $l' = -l$. But the reciprocity principle requires that $B \cos\varepsilon = B' \cos\varepsilon'$ if their surface brightnesses are B and B'. Hence the primed and unprimed areas make equal but opposite contributions to the integral of (l B $\cos\varepsilon$ dA) over the whole visible surface, and the photometric mean longitude $\bar{l}$ is zero. Note that the argument is based only on the reversibility of the light rays and does not require any further assumptions about the photometric function of the surface.†

We can readily correct the geometric central meridian ω to the photometric central meridian ω^*, using quantities tabulated in the Astronomical Ephemeris:

$$\omega^* = \omega - \frac{(A_S - A_E)}{2}, \tag{1}$$

where A_S and A_E are the areocentric right ascensions of the Sun and Earth, respectively. Since the correction term can be as large as $\pm 20°$, its neglect could produce relative misplacements of points by as much as 40° in longitude.

3. Analytic Representation

We can expect three types of regular, intrinsic variation in the brightness of Mars: the phase effect, the rotation effect, and possibility a seasonal effect.

† Stated another way, the reciprocity principle requires dA to send the observer the same amounts of light when it is at l and l'.

https://doi.org/10.1017/S0074180900025493 Published online by Cambridge University Press

Previously, a linear dependence of magnitude on phase angle seemed adequate, although several authors (Young, 1957; de Vaucouleurs, 1960; O'Leary and Rea, 1968) have suggested a sudden brightening on the order of 0.1 mag. at small phase angles. To represent this brightening, we must introduce additional powers of the phase angle. After some unsatisfactory experiments with a cubic, I decided on terms in α^2 and $1/\alpha$; the latter seems to represent the brightening around opposition quite well over the range of the data. Of course, we cannot interpret the constant term as the absolute magnitude at zero phase, or the linear coefficient as the slope of the phase curve in this case.

We can represent the rotational effect analytically as a Fourier series in ω^*. To find the number of terms required for adequate representation, consider a perfectly black planet with a small white spot on one side. As the projected size of the spot varies as $\cos\omega$, the light curve is a half-wave rectified sinusoid if there is no limb darkening, or a half-wave of $\cos^2\omega$ if the spot is a perfect (Lambert) diffuser; Mars is intermediate, between these two cases (Young and Collins, 1971). For the undarkened (lunar) case, the series contains the terms

$$\cos\omega + \frac{4}{3\pi}\cos 2\omega - \frac{4}{15\pi}\cos 4\omega \ldots,$$

where I have normalized the series to the amplitude of the fundamental term. The corresponding series for the Lambert (fully darkened) surface is

$$\cos\omega - \tfrac{3}{16}\pi\cos 2\omega + \tfrac{1}{5}\cos 3\omega - \tfrac{1}{35}\cos 5\omega \ldots.$$

As the visual rotation effect on Mars has an amplitude on the order of a tenth of a magnitude, and we can neglect terms on the order of a hundredth, we see that a fully-darkened Mars would just require the inclusion of the 3ω term. However, the limb darkening is actually less, so we can probably neglect this term as well and use terms in ω and 2ω only.

Two kinds of seasonal effects may be anticipated: a semiannual variation, with a maximum near each solstice, and an annual effect related to the asymmetry of the two hemispheres and the eccentricity of the planet's orbit. Hence we expect to include Fourier series terms in L_S, the areocentric longitude of the Sun measured along the planet's orbit from its vernal equinox. As Mars traverses about 30–40° of L_S from quadrature to opposition, we may expect these seasonal effects to produce slightly different apparent phase coefficients and opposition brightnesses at different oppositions.

We therefore adopt, as equation of condition,

$$\begin{aligned} m_1 = {} & \frac{\mu_{-1}}{\alpha} + m_1(0) + \mu_1\alpha + \mu_2\alpha^2 + a_1\cos\omega^* + b_1\sin\omega^* + \\ & + a_2\cos 2\omega^* + b_2\sin 2\omega^* + c_1\cos L_S + \\ & + d_1\sin L_S + c_2\cos 2L_S + d_2\sin 2L_S, \end{aligned} \tag{2}$$

https://doi.org/10.1017/S0074180900025493 Published online by Cambridge University Press

where m_1 is an observed magnitude reduced to unit distances from both Sun and Earth, μ_i is the coefficient of the ith power phase term, and the other literal coefficients describe the rotational and seasonal effects. We have thus to determine the 12 parameters $(m_1(0), \mu_i, a_1, \ldots, d_2)$ for each color.

4. UBV Observations

There are five series of UBV observations of Mars available for analysis: 21 observations made at Flagstaff in 1954 (Johnson and Gardiner, 1955); 18 at Flagstaff in 1958 (de Vaucouleurs, 1960); 27 at Agassiz Station in 1960–61, reported here for the first time; 76 at Le Houga in 1963–65 (Irvine *et al.*, 1968a); and 124 at Boyden in 1963–65 (Irvine *et al.*, 1968b). Our first concern is to place all the data on the same system, as it has become increasingly clear that systematic errors approaching a tenth of a magnitude can occur in published UBV data (Lawrence and Reddish, 1965; Fernie and Watt, 1967).

Johnson and Gardiner (1955) compared Mars to the stars σ Sgr = HR 7121 and λ Sgr = HR 6913. Both these stars and Mars in 1954 were visible from Flagstaff only at large zenith distances, so that extinction errors are important. Johnson and Gardiner estimated probable errors of 0.04, 0.02, and 0.04 in V, $B-V$, and $U-B$ respectively, in tying the stars to UBV standards, and errors of 0.01 mag. in comparing Mars to the stars. We can now use more accurate UBV data for the two stars to estimate systematic corrections to these Mars data.

Table I gives Johnson and Gardiner's values, together with more extensive measurements made at the Royal Cape Observatory (Cousins and Stoy, 1963) and at Catalina and Tonantzintla (Johnson *et al.*, 1966; the mean of only the four new observations is given, not the value in their Table 2 which includes the 1954 values.) The modern

TABLE I

UBV data for 1954 comparison stars

Star	V	$B-V$	$U-B$	Source
σ Sgr = HR 7121	2.10	−0.20	−0.72	Cousins and Stoy (1963)
	2.07	−0.21	−0.72	Johnson *et al.* (1966)
	2.09	−0.20	−0.72	Adopted values
	2.00	−0.22	−0.76	Johnson and Gardiner (1955)
	+0.09	+0.02	+0.04	Correction to 1954 values
λ SGR = HR 6913	2.845	1.04	+0.91	Cousins and Stoy (1963)
	2.83	1.04	+0.91	Johnson *et al.* (1966)
	2.84	1.04	+0.91	Adopted values
	2.80	1.04	+0.89	Johnson and Gardiner (1955)
	+0.04	0.00	+0.02	Correction to 1954 values

TABLE II

1954 Johnson and Gardiner data

Date	UT	V	$B-V$	$U-B$	α	ω	ω^*	L_S	V_1
1954 April	23.48	−0.530	1.380	0.590	35.12	200.7	218.4	154.0	−0.850
1954 April	27.46	−0.710	1.430	0.600	34.18	156.2	171.8	156.1	−0.930
1954 May	4.46	−0.980	1.460	0.620	32.18	90.9	105.5	159.8	−1.020
1954 May	6.44	−1.030	1.440	0.600	31.52	65.3	79.8	160.8	−1.020
1954 May	11.43	−1.130	1.390	0.560	29.69	15.5	29.1	163.5	−0.990
1954 May	31.38	−1.730	1.390	0.540	19.35	175.1	184.2	174.4	−1.100
1954 June	2.37	−1.830	1.390	0.540	18.04	153.5	162.0	175.5	−1.160
1954 June	4.37	−1.910	1.420	0.550	16.67	135.5	143.4	176.6	−1.190
1954 June	8.35	−2.060	1.460	0.610	13.82	92.6	99.2	178.9	−1.270
1954 June	10.35	−2.060	1.400	0.620	12.32	74.7	80.7	180.0	−1.230
1954 June	19.31	−2.380	1.320	0.660	5.50	340.6	343.3	185.1	−1.420
1954 June	20.39	−2.410	1.300	0.650	4.75	359.8	2.1	185.7	−1.430
1954 June	21.37	−2.460	1.330	0.680	4.14	343.9	345.8	186.3	−1.470
1954 June	29.27	−2.410	1.300	0.610	5.15	238.0	236.8	190.8	−1.370
1954 June	30.32	−2.390	1.300	0.600	5.92	246.7	245.1	191.4	−1.350
1954 July	1.34	−2.360	1.340	0.620	6.72	244.9	242.9	192.0	−1.310
1954 July	2.31	−2.370	1.360	0.620	7.49	225.5	223.1	192.6	−1.320
1954 July	5.35	−2.380	1.370	0.570	9.98	212.9	209.3	194.4	−1.320
1954 July	6.33	−2.360	1.370	0.590	10.79	197.0	193.1	195.0	−1.310
1954 July	7.32	−2.380	1.380	0.600	11.60	184.7	180.4	195.6	−1.330
1954 July	15.23	−2.240	1.350	0.630	17.96	81.8	74.5	200.4	−1.230

TABLE III

1958 de Vaucouleurs data

Date	UT	V	$B-V$	$U-B$	α	ω	ω^*	L_S	V_1
1958 Oct	23.188	−2.034	1.308	0.579	21.32	94.8	104.9	315.5	−1.381
1958 Oct	23.193	−2.027	1.326	0.613	21.31	96.6	106.7	315.5	−1.374
1958 Oct	23.325	−1.994	1.287	0.562	21.21	142.9	153.6	315.6	−1.340
1958 Oct	23.381	−1.993	1.275	0.542	21.17	162.6	172.7	315.6	−1.338
1958 Oct	23.497	−2.074	1.260	0.644	21.08	203.3	213.3	315.7	−1.419
1958 Oct	23.503	−2.062	1.237	0.626	21.08	205.4	215.4	315.7	−1.406
1958 Oct	23.528	−2.070	1.255	0.641	21.06	214.2	224.2	315.7	−1.414
1958 Oct	23.533	−2.037	1.237	0.616	21.05	215.9	225.9	315.7	−1.381
1958 Nov	24.219	−2.147	1.318	0.710	6.83	183.3	180.1	333.4	−1.557
1958 Nov	24.260	−2.119	1.300	0.700	6.87	197.7	194.5	333.4	−1.529
1958 Nov	24.377	−2.050	1.260	0.679	6.97	238.8	235.6	333.5	−1.462
1958 Nov	24.469	−2.018	1.271	0.748	7.05	271.1	267.9	333.5	−1.431
1958 Nov	24.474	−2.010	1.310	0.670	7.05	272.8	269.6	333.5	−1.423
1958 Nov	28.115	−2.098	1.323	0.679	10.14	111.4	106.7	335.5	−1.569
1958 Nov	28.122	−2.106	1.334	0.697	10.14	113.9	109.2	335.5	−1.577
1958 Nov	28.219	−2.081	1.316	0.686	10.22	147.9	143.2	335.6	−1.553
1958 Nov	28.353	−2.122	1.305	0.650	10.33	195.0	190.2	335.6	−1.597
1958 Nov	28.413	−2.082	1.293	0.642	10.38	216.0	211.2	325.7	−1.558

data are quite accordant, but differ appreciably from the 1954 values. Since the Cape values contain at least twice as many observations as the North American ones, and since these stars pass nearly through the zenith at the Cape but must be observed at about 2 air masses by the Arizona observers, we must give practically all the weight to the Cape data. The corrections are much larger for the blue star and increase steadily toward shorter wavelengths, which strongly suggests systematic extinction errors in the 1954 values. Rather than extrapolate the correction to the color of Mars ($B-V\sim 1.4$) I simply adopt the corrections for the redder star ($B-V=1.04$). The corrected values, reduced to unit distance from Sun and Earth, are given in Table II along with the necessary data from the physical ephemeris of Mars.

TABLE IV

Extinction stars and errors for each observing run at Agassiz Station

Dates	Star	V	$B-V$	$U-B$	n	Std
Nov. 18–	α Ari	+1.982	+1.150	+1.129	3	*
Dec. 28, 1960	β Tau	1.639	−0.137	−0.478	5	*
	o Per	3.806	+0.060	−0.765	6	*
	α CMi	0.351	+0.411	−0.013	7	*
	β Cnc	3.533	+1.487	+1.776	5	*
	β Gem	1.150	+0.984	+0.837	11	*
	ν And	4.531	−0.146	−0.590	1	*
	10 Lac	4.898	−0.199	−1.037	1	*
	α Gem	1.569	+0.048	−0.031	9	
	α Tau	0.886	+1.538	+1.934	8	
	R	0.019	0.020	0.016		
	S	0.014	0.020	0.018		
Mar. 4–	β Tau	+1.645	−0.138	−0.482	4	*
Mar. 21, 1961	α CMi	0.352	+0.419	+0.014	6	*
	α Gem	1.580	+0.019	−0.020	7	
	β Gem	1.141	+0.993	+0.861	7	*
	β Cnc	3.507	+1.485	+1.820	5	*
	109 Vir	3.716	+0.004	−0.036	1	*
	ζ Aql	3.002	+0.002	+0.001	4	*
	α Leo	1.360	−0.112	−0.381	3	*
	μ Cnc	5.273	+0.636	+0.240	3	
	47 UMa	5.028	+0.611	+0.127	3	
	α Cr B	2.245	−0.014	−0.053	3	
	ε Cr B	4.158	+1.223	+1.348	4	
	β Ser A	3.669	+0.069	+0.080	2	
	γ Ser	3.868	+0.471	−0.033	2	*
	BD +4° 4048	9.140	+1.486	+1.086	2	*
	BD +13° 3832	8.971	+1.215	+1.081	1	
	BD +13° 3827	8.878	+1.497	+1.429	2	
	χ^1 Ori	4.420	+0.541	+0.126	2	
	BD +13° 3816	9.143	+0.191	−0.278	1	
	BD +13° 3826	7.257	+0.257	+0.248	1	
	R	0.006	0.007	0.017		
	S	0.015	0.017	0.039		

https://doi.org/10.1017/S0074180900025493 Published online by Cambridge University Press

The 1958 observations of de Vaucouleurs (1960) were made on 3 nights with a total of 42 standard star observations. The planet was north of the equator, so extinction errors should not be serious. I accept these data at face value; they are listed in Table III.

My 1960–61 observations were made with the 24-in. Clark reflector at the George R. Agassiz Station of Harvard College Observatory. The reductions were made by the same program used to reduce the later Harvard-NASA observations (Young and Irvine, 1967; Irvine *et al.*, 1968a, b). The observations were made before I realized the importance of the red leak in the *U* filter; the raw *U* data have been corrected by the method of Shao and Young (1965), using constants for the same equipment deduced from observations in 1964–65. This is rather unsatisfactory, but the best that can be done. The average red-leak correction for Mars was about 0.04 mag. The standard stars and standard errors are given for each observing period in Table IV. *R* is the rms residual in the extinction solution for each filter, and hence represents the internal error of a single observation at one air mass. *S* is the rms residual in fitting the instrumental system, reduced to extra-atmospheric magnitudes, to the standard stars indicated by asterisks. The *R* and *S* values in the blue and ultraviolet columns refer to

TABLE V

1960–61 ATY data

Date	UT	V	$B-V$	$U-B$	α	ω	ω^*	L_S	V_1
1960 Nov	18.178	−0.801	1.418	0.549	30.70	352.2	6.4	353.4	−1.052
1960 Nov	18.257	−0.762	1.368	0.517	30.70	20.0	34.1	353.4	−1.011
1960 Nov	18.321	−0.770	1.402	0.499	30.60	42.4	56.5	353.5	−1.018
1960 Nov	18.408	−0.826	1.444	0.533	30.60	72.9	87.0	353.5	−1.073
1960 Nov	31.248	−1.043	1.322	0.539	23.40	259.0	269.9	0.0	−1.113
1960 Dec	19.112	−1.431	1.298	0.544	10.00	51.4	56.3	8.8	−1.353
1960 Dec	19.210	−1.494	1.322	0.524	10.00	85.8	90.7	8.8	−1.415
1960 Dec	19.262	−1.532	1.352	0.513	9.90	104.1	108.9	8.9	−1.453
1960 Dec	19.314	−1.530	1.335	0.521	9.90	122.4	127.2	8.9	−1.451
1960 Dec	19.385	−1.505	1.312	0.535	9.80	147.3	152.1	8.9	−1.426
1960 Dec	19.418	−1.463	1.290	0.549	9.80	158.9	163.7	8.9	−1.384
1960 Dec	23.031	−1.452	1.332	0.519	6.80	347.8	351.2	10.7	−1.367
1960 Dec	23.085	−1.468	1.306	0.499	6.80	6.8	10.2	10.7	−1.383
1960 Dec	23.256	−1.477	1.275	0.474	6.60	66.9	70.2	10.8	−1.392
1960 Dec	23.335	−1.558	1.328	0.511	6.60	94.6	97.9	10.8	−1.473
1960 Dec	23.401	−1.559	1.306	0.437	6.50	117.8	121.0	10.9	−1.474
1960 Dec	27.988	−1.517	1.276	0.523	3.10	288.9	290.3	13.1	−1.443
1960 Dec	28.022	−1.535	1.292	0.563	3.10	300.9	302.3	13.1	−1.462
1960 Dec	28.090	−1.556	1.301	0.540	3.10	324.8	326.2	13.1	−1.483
1960 Dec	28.144	−1.567	1.292	0.546	3.00	343.7	345.1	13.1	−1.494
1961 Mar	4.160	0.075	1.460	0.557	34.40	113.0	97.2	43.6	−1.040
1961 Mar	18.062	0.527	1.432	0.458	36.20	307.1	290.1	49.7	−0.866
1961 Mar	18.110	0.523	1.407	0.581	36.20	323.9	306.9	49.7	−0.871
1961 Mar	18.172	0.501	1.442	0.615	36.20	345.6	328 6	49.8	−0.894
1961 Mar	21.084	0.541	1.475	0.504	36.50	286.5	269.3	51.1	−0.910
1961 Mar	21.156	0.584	1.407	0.588	36.50	311.7	294.5	51.1	−0.868
1961 Mar	21.195	0.553	1.450	0.571	36.50	325.4	308.2	51.1	−0.900

https://doi.org/10.1017/S0074180900025493 Published online by Cambridge University Press

TABLE VI

Le Houga data

Date	UT	V	$B-V$	$U-B$	α	ω	ω^*	L_S	V_1
1964 Aug	31.190	–	1.350	0.570	28.52	4.6	17.5	358.0	−0.990
1964 Sept	9.201	–	1.400	0.570	29.71	281.2	294.8	2.0	−0.950
1964 Sept	10.189	–	1.370	0.540	29.83	267.3	280.9	2.5	−0.950
1964 Sept	23.182	–	1.450	0.590	31.47	138.8	153.4	8.9	−1.020
1964 Dec	8.189	–	1.470	0.640	36.70	128.3	147.4	44.1	−0.920
1964 Dec	8.261	–	1.450	0.600	36.70	153.5	172.6	44.1	−0.950
1964 Dec	9.140	–	1.460	0.630	36.68	101.6	120.7	44.5	−0.960
1965 Jan	11.072	–	1.430	0.610	32.60	126.4	143.8	59.0	−1.000
1965 Jan	11.163	–	1.400	0.590	32.58	158.3	175.7	59.1	−0.980
1965 Feb	3.020	–	1.340	0.530	24.29	257.3	270.4	69.1	−1.040
1965 Feb	3.111	–	1.380	0.560	24.24	289.2	302.3	69.1	−1.030
1965 Feb	4.003	–	1.350	0.570	23.79	242.3	255.1	69.5	−1.010
1965 Feb	4.120	–	1.350	0.540	23.73	283.3	296.1	69.5	−1.060
1965 Feb	4.217	–	1.370	0.590	23.68	317.4	330.2	69.6	−1.100
1965 Feb	5.004	–	1.350	0.530	23.28	233.6	246.1	69.9	−1.030
1965 Feb	5.110	–	1.340	0.550	23.22	270.8	283.3	70.0	−1.050
1965 Feb	10.011	–	1.420	0.620	20.49	191.3	202.3	72.1	−1.210
1965 Feb	10.106	–	1.380	0.580	20.43	224.6	235.6	72.2	−1.080
1965 Feb	24.947	–	1.290	0.540	10.44	36.3	41.9	78.6	−1.330
1965 March	10.023	–	1.280	0.570	2.42	309.8	309.6	84.4	−1.500
1965 March	25.853	–	1.360	0.540	13.34	110.6	103.5	91.3	−1.330
1965 March	25.964	–	1.390	0.590	13.42	149.6	142.5	91.4	−1.320
1965 March	27.826	–	1.320	0.500	14.78	83.6	75.7	92.2	−1.270
1965 March	27.932	–	1.400	0.550	14.86	120.8	112.9	92.3	−1.320
1965 March	28.046	–	1.380	0.590	14.94	160.8	152.8	92.3	−1.310
1965 March	28.115	–	1.380	0.580	14.99	185.1	177.1	92.3	−1.290
1965 March	28.846	–	1.290	0.490	15.52	81.8	73.5	92.7	−1.310
1965 March	28.959	–	1.380	0.560	15.60	121.5	113.2	92.7	−1.300
1965 March	29.046	–	1.400	0.590	15.66	152.0	143.6	92.8	−1.290
1965 March	29.125	–	1.420	0.610	15.72	179.8	171.4	92.8	−1.240
1965 March	29.817	–	1.280	0.490	16.20	62.8	54.1	93.1	−1.250
1965 March	29.923	–	1.340	0.530	16.28	100.0	91.3	93.1	−1.300
1965 March	30.029	–	1.400	0.580	16.35	137.2	128.5	93.2	−1.320
1965 March	30.104	–	1.410	0.560	16.40	163.6	154.8	93.2	−1.280
1965 March	30.937	–	1.340	0.510	16.99	96.1	87.0	93.6	−1.260
1965 March	31.042	–	1.390	0.570	17.06	133.0	123.9	93.6	−1.270
1965 April	3.835	–	1.330	0.510	19.59	24.8	14.3	95.3	−1.140
1965 May	8.853	–	1.300	0.480	34.93	71.7	52.7	111.1	−0.910
1965 May	10.866	–	1.310	0.490	35.42	57.6	38.3	112.0	−0.900
1965 May	10.978	–	1.320	0.480	35.44	96.8	77.5	112.1	−0.970
1965 May	11.863	–	1.330	0.490	35.65	47.1	27.7	112.5	−0.900
1965 May	12.003	–	1.350	0.480	35.68	96.2	76.8	112.6	−0.990
1965 May	12.867	–	1.320	0.500	35.87	39.2	19.7	112.9	−0.860
1965 May	13.866	–	1.360	0.510	36.09	29.4	9.8	113.4	−0.900
1965 May	19.872	–	1.360	0.520	37.23	335.1	314.9	116.2	−0.870
1965 May	21.883	–	1.340	0.510	37.55	320.0	299.6	117.1	−0.840
1965 May	23.902	–	1.300	0.470	37.86	307.7	287.1	118.1	−0.870
1965 May	23.976	–	1.390	0.500	37.87	333.7	313.1	118.1	−0.830
1965 June	17.897	–	1.280	0.480	39.80	67.1	45.8	129.9	−0.840
1965 July	9.878	–	1.460	0.560	39.61	207.7	187.0	140.6	−0.850
1965 July	10.882	–	1.470	0.590	39.57	199.4	178.7	141.1	−0.870

TABLE VII

Boyden data

Date	UT	V	$B-V$	$U-B$	α	ω	ω^*	L_S	V_1
1963 May	28.734	–	1.310	0.510	37.46	39.4	19.2	100.2	−0.830
1963 May	28.815	–	1.280	0.490	37.46	67.8	47.6	100.2	−0.950
1963 May	29.784	–	1.340	0.540	37.42	47.3	27.1	100.6	−0.900
1963 June	2.694	–	1.330	0.500	37.25	337.2	317.0	102.4	−0.880
1963 June	2.796	–	1.370	0.610	37.24	13.0	352.8	102.4	−0.830
1963 June	3.737	–	1.370	0.500	37.19	342.7	322.5	102.9	−0.890
1963 June	8.760	–	1.260	0.460	36.91	302.4	282.3	105.1	−0.850
1963 June	9.740	–	1.200	0.440	36.86	285.8	265.8	105.6	−0.820
1963 June	14.740	–	1.340	0.550	36.51	237.4	217.5	107.8	−0.830
1963 June	15.732	–	1.350	0.510	36.44	224.9	205.0	108.3	−0.900
1963 June	23.791	–	1.320	0.590	35.79	167.9	148.4	112.0	−0.910
1963 June	23.803	–	1.270	0.610	35.79	172.1	152.6	112.0	−0.860
1963 June	24.707	–	1.360	0.510	35.71	128.8	109.3	112.4	−1.000
1963 June	24.801	–	1.290	0.640	35.70	161.7	142.2	112.4	−0.900
1965 April	12.713	–	1.250	0.560	24.84	261.4	248.0	99.3	−1.050
1965 April	12.805	–	1.240	0.420	24.89	293.7	280.3	99.3	−1.060
1965 April	12.918	–	1.330	0.480	24.95	333.4	319.9	99.4	−1.040
1965 April	27.707	–	1.380	0.520	31.53	122.6	105.5	106.0	−1.070
1965 April	27.801	–	1.410	0.560	31.57	155.5	138.4	106.1	−1.080

B and U magnitudes, not colors, as the reduction is all done in terms of magnitudes. The systematic error in a run should be on the order of S divided by the square root of the number of standard stars; this is generally less than 0.01 mag. The random error of one observation should be on the order of R times the air mass, or typically 0.02 or 0.03 mag. Table V gives the observations and parameters as in Tables II and III.

The Harvard-NASA photometry has been described by Irvine *et al.* (1968a, b). These data are so numerous that we can afford to reject observations affected by clouds or with R or S greater than 0.03 for B or V, or 0.05 for U. The remaining data are listed in Tables VI and VII. The B and U magnitudes have been converted to $B-V$ and $U-B$ colors for consistency with the other data. Note that only the magnitude at unit distance (V_1) is given, not V.

We may now hope that all the data are on the same photometric system. However, we must fear that substantial systematic errors remain, particularly in U and B. There is first of all the problem of correcting so red an object for atmospheric extinction. The ultraviolet extinction corrections applied to all the observations after 1959 may differ systematically from those used by Johnson, but this difference should not exceed about 0.03 mag. A more serious problem arises from the fact that Mars does not resemble a normal star or a black body in the $U-B$, $B-V$ diagram (Figure 1); it corresponds roughly to a late B star seen through about 1.5 mag. of interstellar reddening ($\sim$4.5 mag. of visual absorption). Relative to main-sequence stars of similar $B-V$ color, Mars appears to have an 'ultraviolet excess' of about 0.6 mag. Schmidt-Kaler (1961) has shown that the normal transformation of instrumental systems to UBV, which is largely based on unreddened stars, often gives incorrect values for

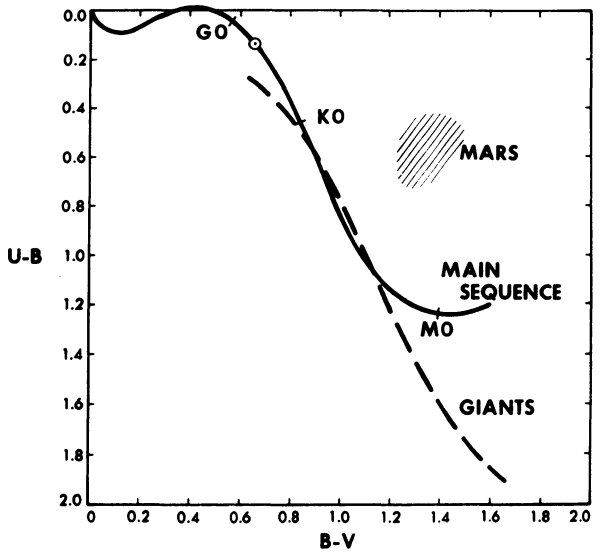

Fig. 1. Location of Mars data in the $(U-B)$, $(B-V)$ plane.

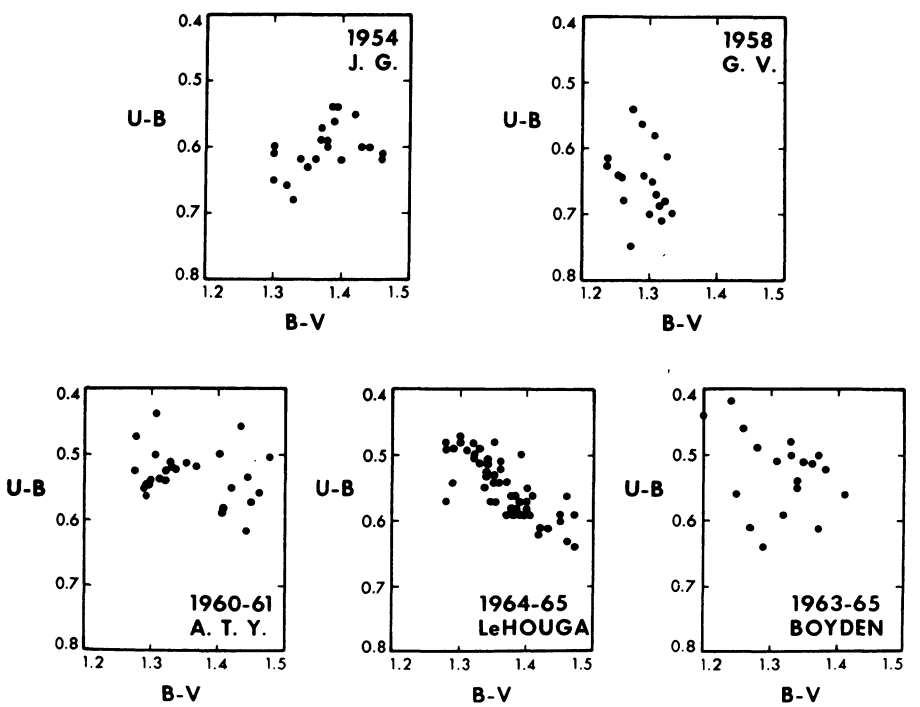

Fig. 2. Distribution of different observers' Mars data in the color-color diagram.

https://doi.org/10.1017/S0074180900025493 Published online by Cambridge University Press

heavily-reddened objects. Systematic errors in $(B-V)$ exceeding a tenth of a magnitude per magnitude of reddening can occur, so we may expect systematic errors in $(B-V)$ of 0.15 mag. for Mars. The transformation difficulties in the ultraviolet are even more severe. Basically, the UBV 'system' is not defined for objects like Mars.

In fact, Figure 2 suggests that systematic errors of the expected size do exist. We must therefore include a systematic correction term for each set of observations in fitting the data to Equation (2). This greatly weakens the determination of seasonal effects, but appears necessary because of the impossibility of placing Mars uniquely on a UBV-type system.

5. Analysis of the Data

The geometric data in Tables II, III, V, VI, and VII are approximately on the modern system defined in U.S. Naval Observatory Circular 98 (Meiller, 1964), which has been adopted by the Astronomical Ephemeris beginning with 1968. Because the new tabulation for past oppositions only goes to phase angles of about 25°, the old Ephemeris values for each opposition have been systematically corrected by the values given in Table VIII.

TABLE VIII

Corrections to be added to AE values for reduction to new physical ephemeris of Mars

Year	$\Delta\omega$	ΔL_S
1954	−0°.6	+3°.8
1958	−1.1	+3.8
1960–61	+0.2	+3.8
1963	0.0	+3.8
1965	−0.4	+3.8

To see whether the data are well enough distributed to separate the phase, rotational, and seasonal effects, I have plotted their distribution in ω^* and L_S (see Figure 3). Open symbols mark points with $i \leqslant 12°$. Although there are gaps in L_S, the distribution appears fairly satisfactory.

I therefore fit the data by least squares to Equation (2), determining the four additional zero-point adjustments required to reduce all series to the Le Houga system. (I adopt the Le Houga data as standard not only because they are most numerous, but also because they show the best-defined color-color relation in Figure 2.) The least-squares fits were performed in double precision, using the Los Alamos least-squares routine LEAST.

Initially, all observations were given equal weight, but some data sets are clearly better than others, so the standard error of one observation was computed from the initial residuals for each set and used to determine an average weight. The solution was repeated, weighing each set accordingly.

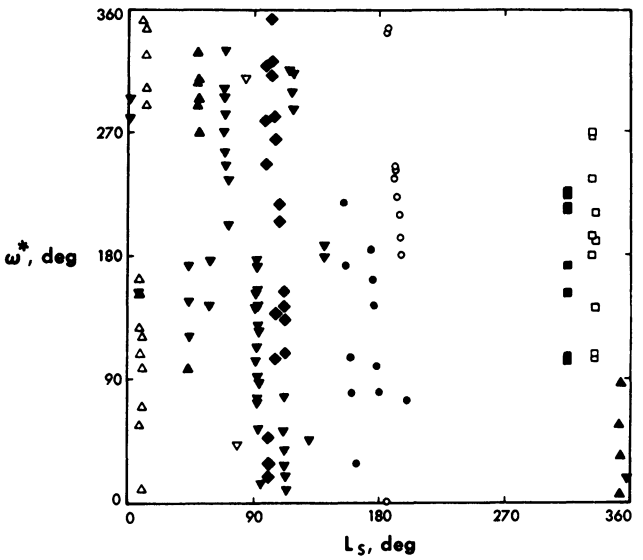

Fig. 3. Distribution of Mars data with L_S and ω^*. Observations at phase angles less than 12° are indicated by open circles. Note that small-phase points occur at all central meridians, and that data are well-distributed in ω^* at each L_S covered.

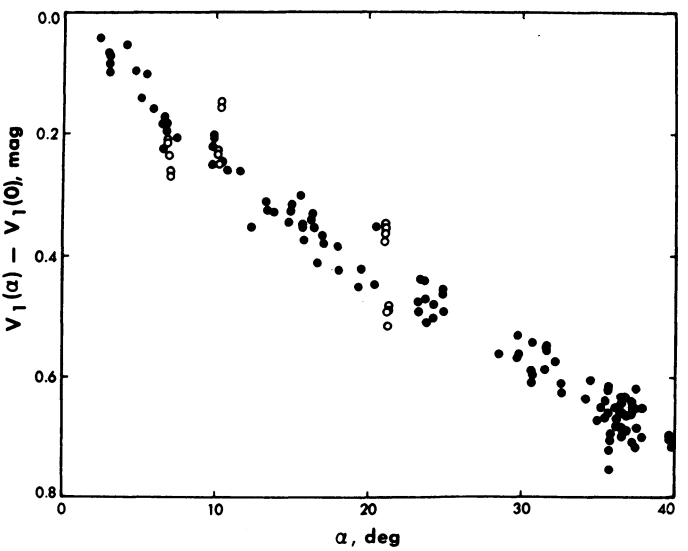

Fig. 4. V magnitudes of Mars, approximately corrected for rotation and seasonal effects, as a function of phase. The 1958 data are indicated by open circles; note their large scatter and systematic displacement from night to night.

https://doi.org/10.1017/S0074180900025493 Published online by Cambridge University Press

The weights for most sets differ by a factor of 2 or less, but the 1958 data have an unusually low weight. Inspection of these residuals in the phase and L_S diagrams (Figures 4 and 5) shows large systematic shifts from night to night, as well as large scatter within each night. Because of these large systematic effects, I have tried solutions both with and without the 1958 data. Unfortunately, the 1958 data have a large influence on the seasonal effect in spite of their low weight. I have therefore tried solutions both with and without the seasonal effects. Thus, there are four solutions altogether: (I) all data, full solution; (II) all data, no seasonal effect; (III) no 1958 data, no seasonal effect; and (IV) full solution without 1958 data.

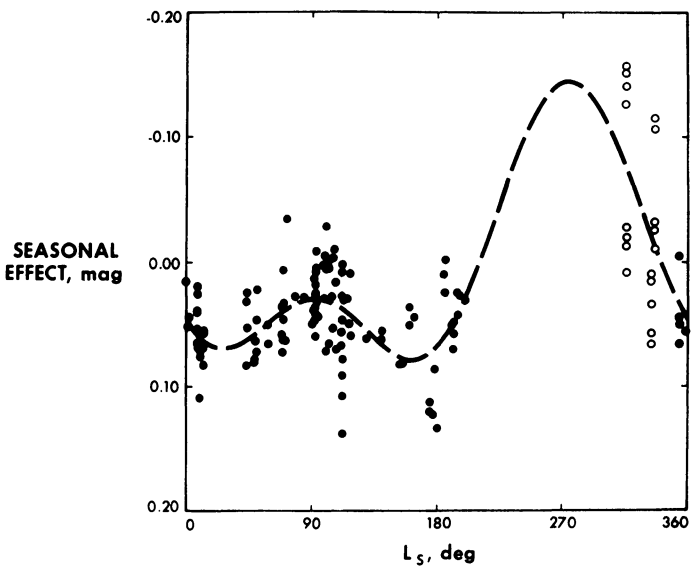

Fig. 5. V magnitudes of Mars, approximately corrected for rotation and phase effects, as a function of Martian season. The 1958 data are open circles. The least-squares seasonal effect is represented by a dashed line. The influence of the 1958 data on the determination of the seasonal effect is obvious.

Tables IX through XII give the results of the (weighted) solutions I through IV, respectively. Each solution has been done separately for the V, B, and U magnitudes and the $(B-V)$ and $(U-B)$ colors. The coefficients (and their corresponding terms) are listed in order from Equation (2). The zero-point term $Z_{(\text{set})}$ is such that

$$m_{(\text{set})} = m_{(\text{Le Houga})} + Z_{(\text{set})}, \tag{3}$$

i.e., it appears on the right-hand side of Equation (2) as an additive constant. The standard errors of all coefficients and zero points are also given. The tabulated weights, *used* in each solution, are inversely proportional to the error variances (mean-square residuals) found from the corresponding unweighted solution; but the tabulated rms residuals are those from the weighted solution. Thus the weights are not quite proportional to the inverse squares of the rms residuals given below them in

TABLE IX

Solution I: full solution, all data

Quantity		V	B	U	$B-V$	$U-B$
Phase coefficients (and terms):						
μ_{-1}	$(1/\alpha)$	−0.235	−0.218	−0.237	−0.087	+0.012
		±0.105	±0.166	±0.248	±0.130	±0.126
$m_1(0)$	(1)	−1.508	−0.286	+0.285	+1.254	+0.553
		±0.042	±0.061	±0.087	±0.046	±0.049
μ_1	(α)	+0.0171	+0.0256	+0.0211	+0.0047	−0.0023
		±0.0031	±0.0045	±0.0065	±0.0034	±0.0036
μ_2	(α^2)	−0.000040	−0.000164	−0.000070	−0.000056	+0.000046
		±0.000062	±0.000089	±0.000128	±0.000067	±0.000070
Rotational coefficients (and terms):						
a_1	$(\cos\omega^*)$	+0.022	−0.001	−0.010	−0.018	−0.015
		±0.004	±0.006	±0.009	±0.005	±0.005
b_1	$(\sin\omega^*)$	−0.051	−0.037	−0.032	+0.013	+0.002
		±0.004	±0.006	±0.009	±0.004	±0.004
a_2	$(\cos 2\,\omega^*)$	0.000	+0.011	+0.018	+0.004	+0.016
		±0.004	±0.006	±0.008	±0.004	±0.004
b_2	$(\sin 2\,\omega^*)$	+0.017	−0.008	−0.020	−0.022	−0.013
		±0.004	±0.006	±0.009	±0.004	±0.004
Seasonal coefficients (and terms)						
c_1	$(\cos L_S)$	−0.010	−0.033	−0.014	−0.015	+0.011
		±0.021	±0.030	±0.042	±0.022	±0.023
d_1	$(\sin L_S)$	+0.085	+0.128	+0.163	+0.078	+0.038
		±0.026	±0.036	±0.048	±0.020	±0.027
c_2	$(\cos 2\,L_S)$	+0.056	+0.090	+0.111	+0.050	+0.025
		±0.018	±0.026	±0.036	±0.017	±0.019
d_2	$(\sin 2\,L_S)$	+0.006	+0.041	+0.077	+0.035	+0.035
		±0.011	±0.015	±0.022	±0.011	±0.012
Zero points for:						
Flagstaff, 1954		+0.001	+0.007	+0.075	+0.015	+0.054
		±0.037	±0.051	±0.071	±0.037	±0.040
Flagstaff, 1958		−0.117	−0.091	+0.053	+0.051	+0.144
		±0.034	±0.049	±0.069	±0.032	±0.036
Agassiz Station, 1960–61		−0.039	−0.027	−0.088	−0.002	−0.053
		±0.010	±0.017	±0.025	±0.013	±0.013
Le Houga, 1964–65		(0.000)	(0.000)	(0.000)	(0.000)	(0.000)
Boyden, 1963–65		+0.014	−0.040	−0.040	−0.051	+0.001
		±0.012	±0.014	±0.024	±0.013	±0.013
Weights used (and rms residuals):						
Flagstaff, 1954		1.143	1.338	1.871	1.832	1.024
		(0.034)	(0.042)	(0.053)	(0.024)	(0.044)
Flagstaff, 1958		0.360	0.441	0.596	1.821	0.788
		(0.066)	(0.084)	(0.099)	(0.022)	(0.047)
Agassiz Station, 1960–61		2.213	1.149	1.020	0.883	0.861
		(0.023)	(0.046)	(0.071)	(0.043)	(0.045)
Le Houga, 1964–65		2.578	1.854	1.710	1.363	2.757
		(0.021)	(0.033)	(0.050)	(0.029)	(0.019)
Boyden, 1963–65		0.745	1.067	0.691	0.535	0.589
		(0.044)	(0.047)	(0.086)	(0.051)	(0.050)

TABLE X

Solution II: all data, no seasonal effect

Quantity	V	B	U	$B-V$	$U-B$
Phase coefficients (and terms):					
μ_{-1} $(1/\alpha)$	−0.282	−0.249	−0.221	−0.124	+0.084
	±0.097	±0.159	±0.250	±0.125	±0.138
$m_1(0)$ (1)	−1.436	−0.206	+0.360	+1.308	+0.543
	±0.033	±0.053	±0.079	±0.038	±0.045
μ_1 (α)	+0.0135	+0.0221	+0.0200	+0.0029	0.0000
	±0.0024	±0.0037	±0.0056	±0.0027	±0.0031
μ_2 (α^2)	+0.000041	−0.000080	−0.000037	−0.000021	−0.000001
	±0.000044	±0.000069	±0.000105	±0.000050	±0.000058
Rotational coefficients (and terms):					
a_1 $(\cos\omega^*)$	+0.020	−0.006	−0.016	−0.023	−0.018
	±0.004	±0.007	±0.010	±0.005	±0.006
b_1 $(\sin\omega^*)$	−0.051	−0.042	−0.042	+0.008	−0.005
	±0.004	±0.006	±0.009	±0.005	±0.005
a_2 $(\cos 2\omega^*)$	0.000	+0.012	+0.016	+0.004	+0.014
	±0.004	±0.006	±0.009	±0.004	±0.005
b_2 $(\sin 2\omega^*)$	+0.015	−0.013	−0.031	−0.028	−0.017
	±0.004	±0.006	±0.010	±0.005	±0.005
Zero points for					
Flagstaff, 1954	+0.020	+0.066	+0.119	+0.039	+0.049
	±0.010	±0.014	±0.018	±0.009	±0.011
Flagstaff, 1958	−0.196	−0.244	−0.147	−0.055	+0.090
	±0.016	±0.022	±0.031	±0.012	±0.014
Agassiz Station, 1960–61	−0.028	−0.001	−0.024	+0.017	−0.018
	±0.007	±0.012	±0.019	±0.010	±0.011
Le Houga, 1964–65	(0.000)	(0.000)	(0.000)	(0.000)	(0.000)
Boyden, 1963–65	+0.003	−0.068	−0.090	−0.070	−0.021
	±0.011	±0.013	±0.024	±0.013	±0.013
Weights used (and rms residuals):					
Flagstaff, 1954	0.867	1.161	1.987	1.968	1.059
	(0.041)	(0.049)	(0.057)	(0.027)	(0.047)
Flagstaff, 1958	0.374	0.398	0.483	0.961	0.704
	(0.069)	(0.104)	(0.135)	(0.039)	(0.057)
Agassiz Station, 1960–61	2.339	1.415	1.291	0.934	1.031
	(0.023)	(0.043)	(0.064)	(0.042)	(0.042)
Le Houga, 1964–65	2.276	1.623	1.341	1.405	1.658
	(0.023)	(0.037)	(0.066)	(0.030)	(0.029)
Boyden, 1963–65	0.804	1.210	0.845	0.550	0.703
	(0.043)	(0.047)	(0.088)	(0.054)	(0.051)

https://doi.org/10.1017/S0074180900025493 Published online by Cambridge University Press

TABLE XI

Solution III: all data but 1958; no seasonal effect

Quantity		V	B	U	$B-V$	$U-B$
Phase coefficients (and terms):						
μ_{-1}	$(1/\alpha)$	−0.218	−0.083	+0.180	+0.091	+0.310
		±0.099	±0.153	±0.236	±0.126	±0.132
$m_1(0)$	(1)	−1.469	−0.280	+0.177	+1.214	+0.431
		±0.035	±0.053	±0.080	±0.042	±0.046
μ_1	(α)	+0.0161	+0.0278	+0.0339	+0.0100	+0.0084
		±0.0024	±0.0037	±0.0057	±0.0030	±0.0033
μ_2	(α^2)	−0.000006	−0.000185	−0.000294	−0.000149	−0.000154
		±0.000045	±0.000068	±0.000106	±0.000055	±0.000060
Rotational coefficients (and terms):						
a_1	$(\cos\omega^*)$	+0.018	−0.010	−0.027	−0.027	−0.023
		±0.004	±0.006	±0.010	±0.005	±0.006
b_1	$(\sin\omega^*)$	−0.052	−0.042	−0.043	+0.008	−0.001
		±0.004	±0.006	±0.009	±0.005	±0.005
a_2	$(\cos 2\omega^*)$	+0.002	+0.017	+0.033	+0.010	+0.021
		±0.004	±0.006	±0.009	±0.005	±0.005
b_2	$(\sin 2\omega^*)$	+0.017	−0.010	−0.026	−0.026	−0.018
		±0.004	±0.006	±0.010	±0.025	±0.005
Zero points for:						
Flagstaff, 1954		+0.022	+0.068	+0.127	+0.044	+0.058
		±0.010	±0.013	±0.020	±0.009	±0.013
Agassiz Station, 1960–61		−0.023	+0.008	−0.002	+0.027	−0.005
		±0.007	±0.011	±0.017	±0.009	±0.010
Le Houga, 1964–65		(0.000)	(0.000)	(0.000)	(0.000)	(0.000)
Boyden, 1963–65		+0.003	−0.067	−0.089	−0.069	−0.020
		±0.010	±0.013	±0.022	±0.013	±0.012
Weights used (and rms residuals):						
Flagstaff, 1954		0.711	0.766	0.861	1.314	0.637
		(0.039)	(0.050)	(0.077)	(0.033)	(0.060)
Agassiz Station, 1960–61		1.340	1.025	1.249	1.052	1.120
		(0.025)	(0.044)	(0.061)	(0.039)	(0.038)
Le Houga, 1964–65		1.839	1.422	1.318	1.518	1.851
		(0.022)	(0.035)	(0.057)	(0.027)	(0.025)
Boyden, 1963–65		0.558	0.885	0.720	0.528	0.709
		(0.043)	(0.046)	(0.082)	(0.054)	(0.048)

TABLE XII

Solution IV: all data but 1958; full solution

Quantity		V	B	U	B − V	U − B
Phase coefficients (and terms):						
μ_1	$(1/\alpha)$	−0.208	−0.064	+0.199	+0.147	+0.201
		±0.107	±0.162	±0.232	±0.133	±0.124
$m_1(0)$	(1)	−1.522	−0.319	+0.172	+1.198	+0.509
		±0.041	±0.060	±0.089	±0.048	±0.049
μ_1	(α)	+0.0184	+0.0296	+0.0342	+0.0111	+0.0040
		±0.0031	±0.0046	±0.0067	±0.0037	±0.0036
μ_2	(α^2)	−0.000066	−0.000226	−0.000287	−0.000159	−0.000061
		±0.000062	±0.000089	±0.000133	±0.000073	±0.000071
Rotational coefficients (and terms):						
a_1	$(\cos\omega^*)$	+0.021	−0.004	−0.018	−0.023	−0.019
		±0.004	±0.007	±0.010	±0.005	±0.005
b_1	$(\sin\omega^*)$	−0.052	−0.036	−0.029	+0.015	+0.006
		±0.004	±0.006	±0.009	±0.005	±0.004
a_2	$(\cos 2\omega^*)$	+0.001	+0.016	+0.035	+0.011	+0.021
		±0.004	±0.005	±0.008	±0.005	±0.004
b_2	$(\sin 2\omega^*)$	+0.019	−0.006	−0.020	−0.024	−0.016
		±0.004	±0.006	±0.009	±0.005	±0.004
Seasonal coefficients (and terms):						
c_1	$(\cos L_S)$	−0.015	−0.033	−0.028	−0.016	−0.004
		±0.021	±0.030	±0.045	±0.024	±0.023
d_1	$(\sin L_S)$	+0.088	+0.069	+0.016	−0.009	−0.043
		±0.028	±0.043	±0.061	±0.032	±0.037
c_2	$(\cos 2L_S)$	+0.059	+0.055	+0.031	+0.001	−0.013
		±0.019	±0.028	±0.041	±0.023	±0.022
d_2	$(\sin 2L_S)$	+0.008	+0.040	+0.079	+0.032	+0.040
		±0.010	±0.016	±0.023	±0.012	±0.012
Zero points for:						
Flagstaff, 1954		−0.007	+0.012	+0.068	+0.022	+0.034
		±0.036	±0.052	±0.078	±0.041	±0.041
Agassiz Station, 1960–61		−0.036	−0.012	−0.043	+0.022	−0.032
		±0.010	±0.016	±0.023	±0.013	±0.012
Le Houga, 1964–65		(0.000)	(0.000)	(0.000)	(0.000)	(0.000)
Boyden, 1963–65		+0.015	−0.047	−0.057	−0.061	−0.006
		±0.012	±0.014	±0.023	±0.014	±0.013
Weights used (and rms residuals):						
Flagstaff, 1954		0.911	0.826	0.830	1.278	0.680
		(0.033)	(0.046)	(0.071)	(0.031)	(0.051)
Agassiz Station, 1960–61		1.479	1.105	1.416	1.318	1.044
		(0.023)	(0.040)	(0.052)	(0.032)	(0.036)
Le Houga, 1964–65		1.805	1.476	1.506	1.447	2.638
		(0.021)	(0.033)	(0.048)	(0.028)	(0.018)
Boyden, 1963–65		0.503	0.842	0.658	0.544	0.605
		(0.044)	(0.045)	(0.078)	(0.050)	(0.046)

https://doi.org/10.1017/S0074180900025493 Published online by Cambridge University Press

parentheses. The zero point for Le Houga is defined as zero, as it is the reference system.

Although I have shown in Section 3 that the terms used should represent the rotational effect quite accurately, there is no reason to believe that the terms used to represent the phase and seasonal variations are an accurate representation of these effects; they are merely analytically convenient interpolation formulae. Each effect can be truly displayed by plotting the sum of the computed least-squares value and the residual for each observational datum, however; this sum is simply the observed value *minus* the analytical representation of all other effects. Thus, we need only

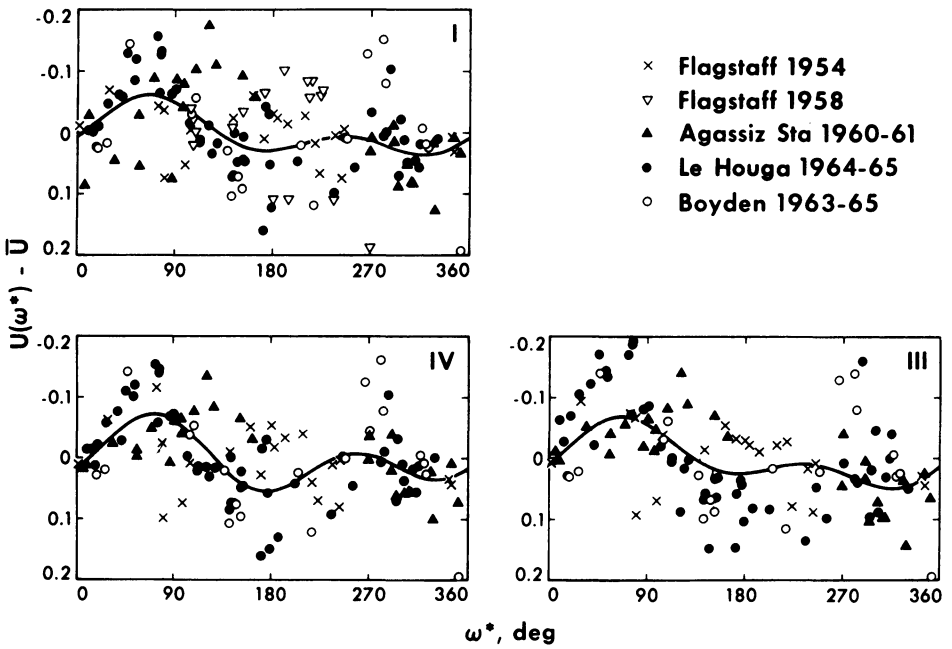

Fig. 6. Ultraviolet rotational effect, from Solutions I–IV (see Tables IX–XII). The formats of Figures 6–14 are similar: the upper two plots (Solutions I and II) contain the 1958 data, which the lower two (Solutions III and IV) exclude; and the left two solutions (I and IV) include the seasonal terms, which are omitted from the right two (Solutions II and III). In the present case, the scatter for Solution II was too large to fit in the space available, so it has been omitted.

require that the interpolation formula represents the bulk of each effect, so that the remainder does not introduce appreciable scatter or systematic error into the graphs for the other effects.

The graphs of the rotational, phase, and seasonal effects in U, B, and V (constructed as described above) are given in Figures 6 through 14. The least-squares representation for each effect is drawn in for comparison. As we should expect, the least-squares formula fits the rotational effect very well, but the reader may choose to draw other lines through the points that give the phase and seasonal effects.

https://doi.org/10.1017/S0074180900025493 Published online by Cambridge University Press

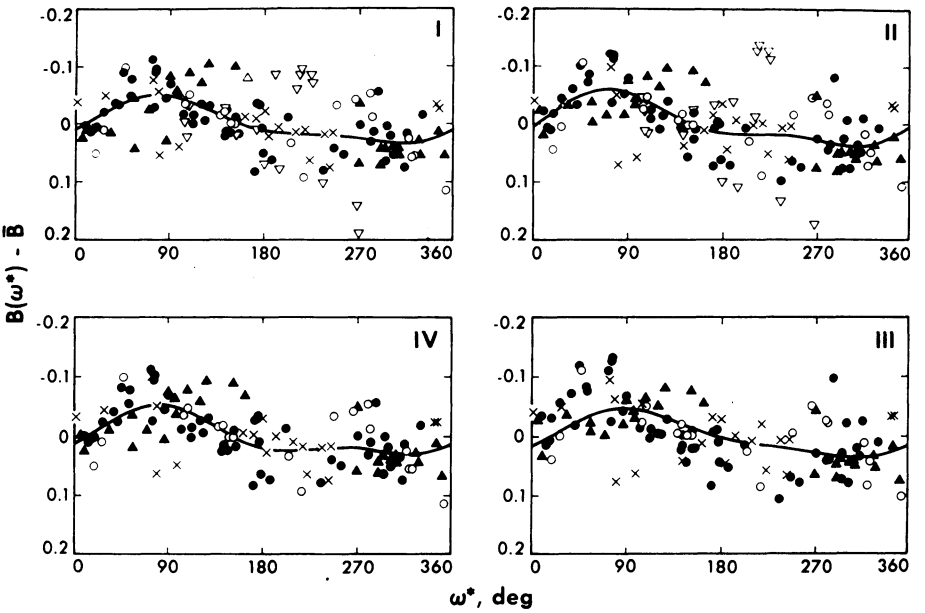

Fig. 7. Blue rotational effect. (See legend and caption of Figure 6 for explanation.)

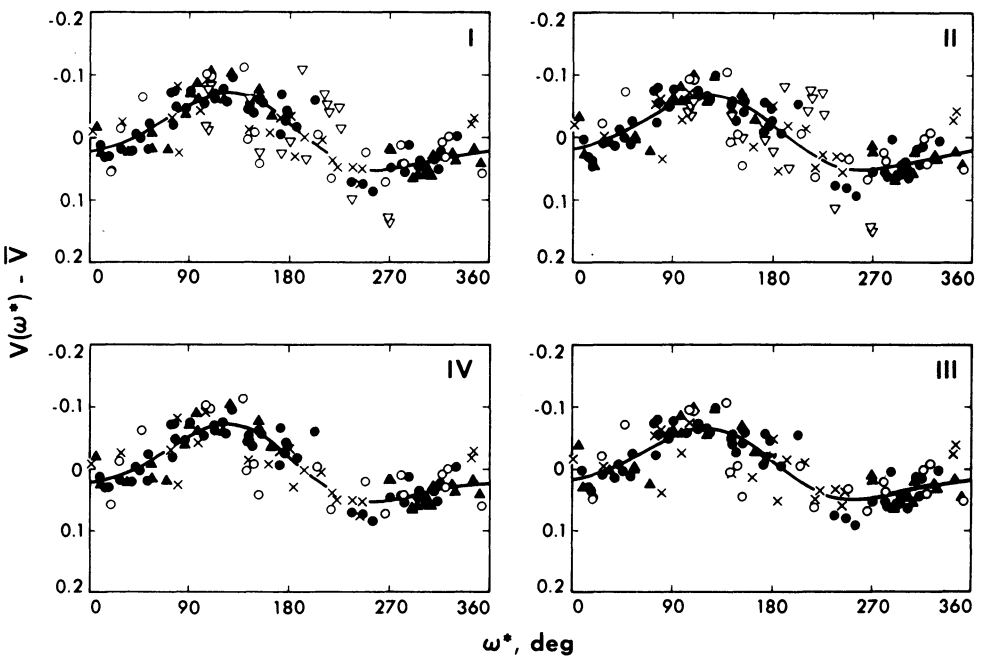

Fig. 8. Visual rotational effect. (See Figure 6.)

https://doi.org/10.1017/S0074180900025493 Published online by Cambridge University Press

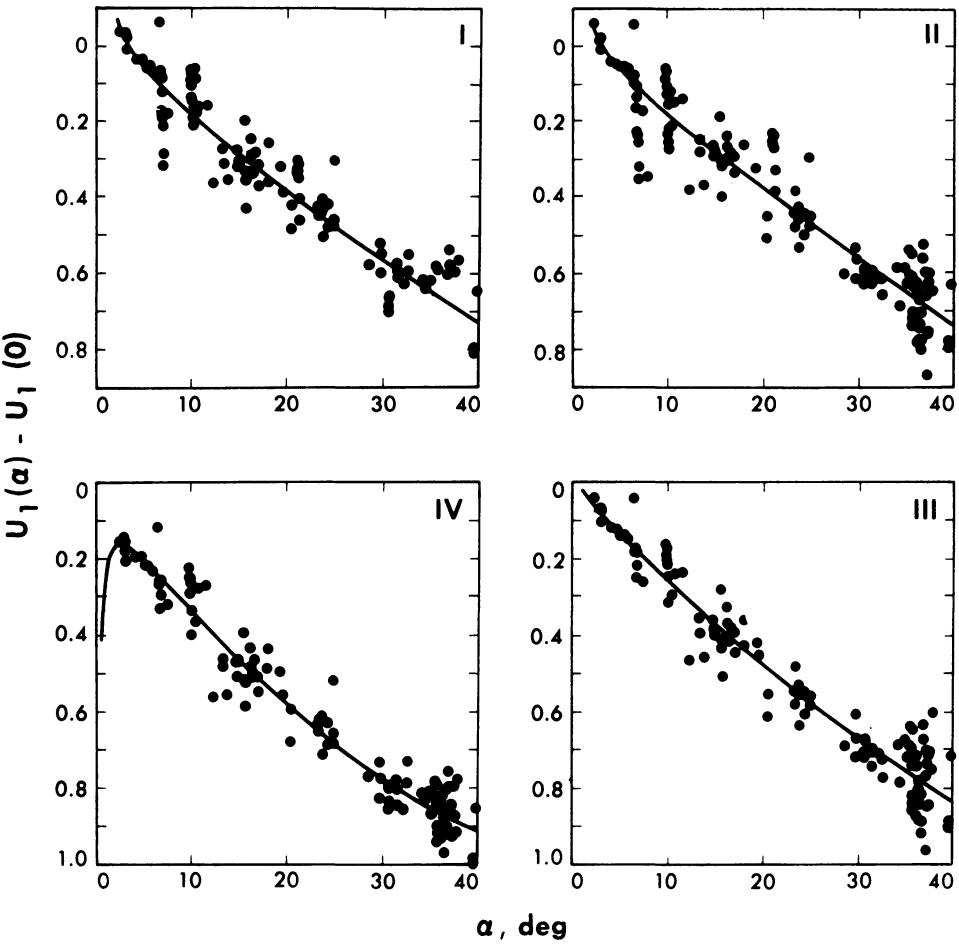

Fig. 9. Ultraviolet phase effect. (See Figure 6.)

6. Discussion

6.1. The rotational effect

The rotation curve is very well determined in visual light (Figure 8), and is not in doubt by as much as 0.01 mag. The large volume of data analyzed here shows an appreciable rotational effect even in blue (Figure 7) and ultraviolet (Figure 6) light; the progressive changes in the curves with changing wavelength confirm the reality of these results. The roughly constant longitude of the maximum suggests that the surface features retain appreciable contrast even in the ultraviolet; the shift toward lower longitudes at shorter wavelengths may be due to the increasing influence of the North Polar Cap, which is displaced toward longitude 30°.

https://doi.org/10.1017/S0074180900025493 Published online by Cambridge University Press

6.2. The seasonal effect

The reality of the seasonal effect may be judged by comparing Solutions II and III (no seasonal effect) with Solutions I and IV, respectively. The effect is clearly present in the ultraviolet (Figure 12), and probably present in the blue data (Figure 13), whether the 1958 observations are included or not. Furthermore, the similar shape in all wavelengths, and the steady increase in amplitude toward the ultraviolet, strongly suggest a real effect.

However, the sign of the effect is puzzling if it represents real seasonal changes on Mars. We would expect the planet to appear brightest when the polar caps appear largest, as the caps are the brightest part of the disc, especially in the ultraviolet. Unfortunately, the observed effect is brightest after the Martian solstices, when the caps have disappeared, and faintest after the equinoxes, when the visible cap is large. Two possible explanations are that (a) we are observing seasonal changes of 10 to 20%

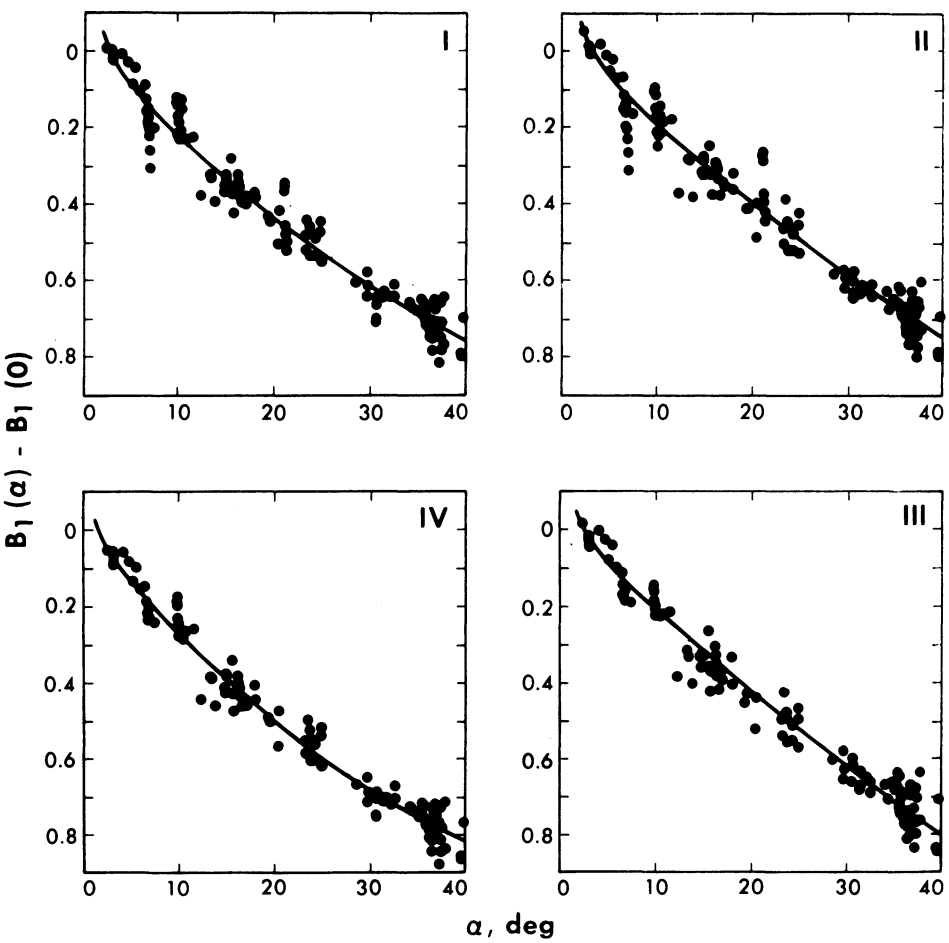

Fig. 10. Blue phase effects. (See Figure 6.)

https://doi.org/10.1017/S0074180900025493 Published online by Cambridge University Press

in the brightness of the bright areas, which contribute most of the observed light in any case, or that (b) the light contributed by Martian aerosols increases after the solstices, due either to an increase in atmospheric pressure (if the caps are CO_2) or to an increase in wind speed at the peak of the annual temperature cycle. The 1971 dust storm, which peaked near $L_S = 280°$, supports this interpretation.

Alternatively, one may imagine that the effect, though real, is in the data but not on Mars – e.g., some systematic, time-dependent error in the Le Houga photometer, due perhaps to secular or (terrestrial) seasonal effects. However, inspection of the zero-point terms in the tables shows no regular, progressive change with wavelength, so the regular progression with wavelength argues against such an explanation.

The maximum at $L_S = 300°$ (near perihelion) is alarming. However, it appears whether the 1958 data are included or not (compare Solution I with Solution IV, or II with III). Furthermore, the inclusion of the seasonal effect reduces not only the

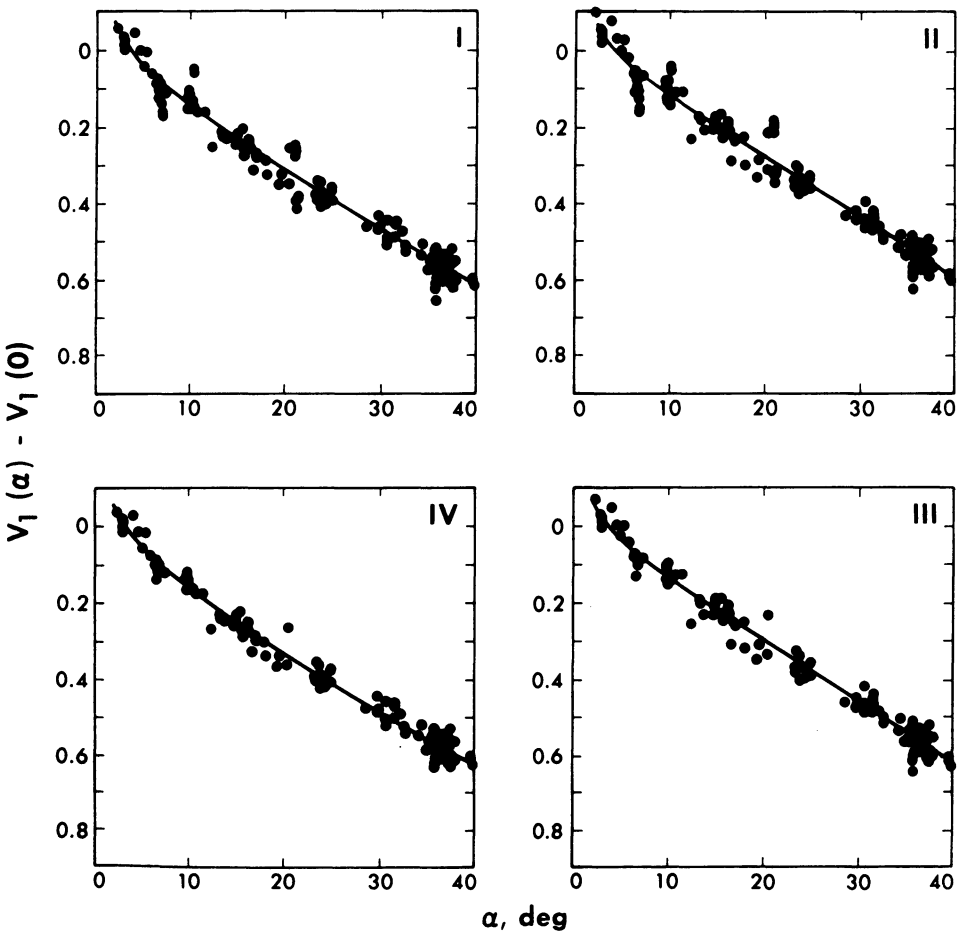

Fig. 11. Visual phase effect. (See Figure 6.)

https://doi.org/10.1017/S0074180900025493 Published online by Cambridge University Press

scatter of the 1958 data, but also the large zero-point terms. This is indirect evidence that the maximum, though uncertain in amplitude, is probably real. The actual shape and size of the maximum cannot be determined until a homogeneous set of good observations covering the gap in L_S (200°–350°) is available. However, the shape of the seasonal effect in this gap is not needed for the correction of the existing data, so it should not greatly influence the determination of the phase and rotational effects in the present work.

6.3. Phase effect

All the curves show a sharp brightening at small phase angles, except for Solutions III and IV in the ultraviolet. The shapes of the phase curves are sensitive to the inclusion of the seasonal effect: they bend up more at large phase angles (30°–40°) in the solutions that include the seasonal effect (I and IV) than in those that do not (II and III).

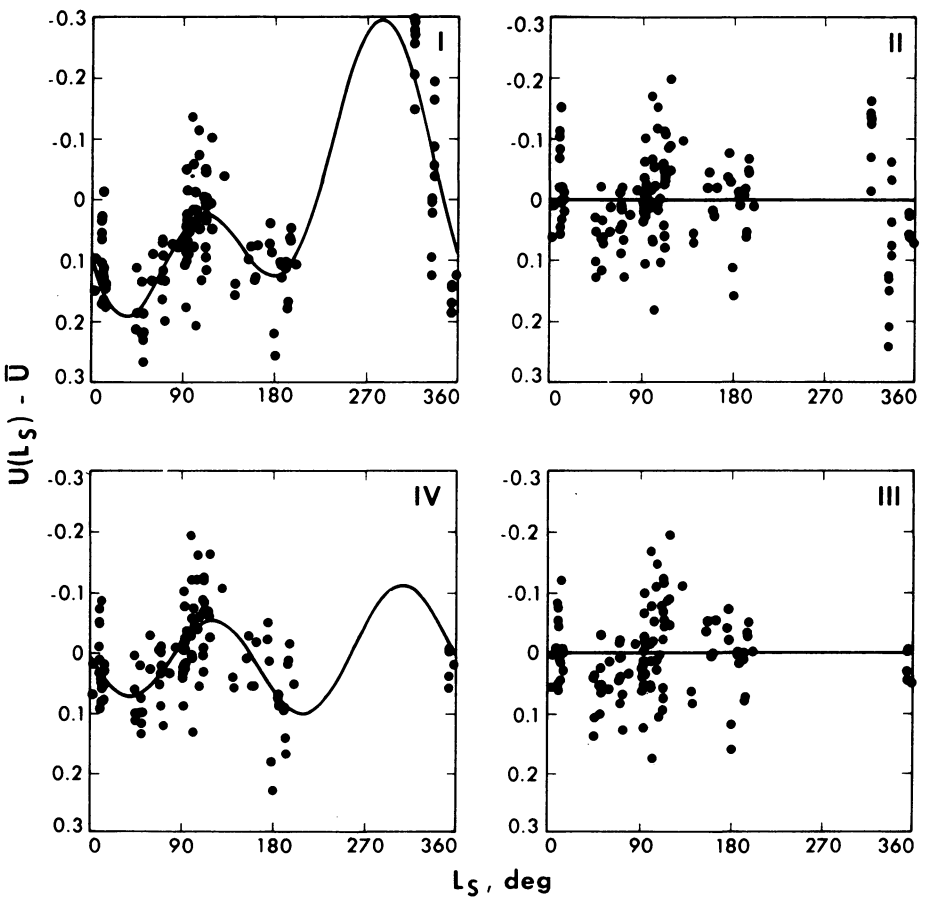

Fig. 12. Ultraviolet seasonal effect. (See Figure 6.)

https://doi.org/10.1017/S0074180900025493 Published online by Cambridge University Press

I have argued above that the seasonal effects are probably real (whether Martian or terrestrial), so I favor the more strongly-curved Solutions I and IV.

Because of the uncertainty in the seasonal effect, and the mutual dependence of the phase and seasonal effects, the uncertainty in the phase effects remains fairly large. However, the uncertainty in the phase effect is not as large as would appear from the standard errors of the coefficients, because the terms used are not linearly independent; thus a small change of one coefficient would be largely compensated by changes in the others. Only in the rotational effect, where the terms are linearly independent and the observations well distributed, do the tabulated errors really indicate the uncertainty of the curve. A realistic estimate of the uncertainty near the middle ($\alpha = 20°$) of the phase curve would be 0.02 mag, in V, 0.03 mag. in B, and 0.05 mag. in U; at the ends ($\alpha \approx 0°$ or 40°) the uncertainty is about twice as big. Thus the slopes near $\alpha = 20°$ are still uncertain by about 0.001 mag deg^{-1} in V, and more in B and U.

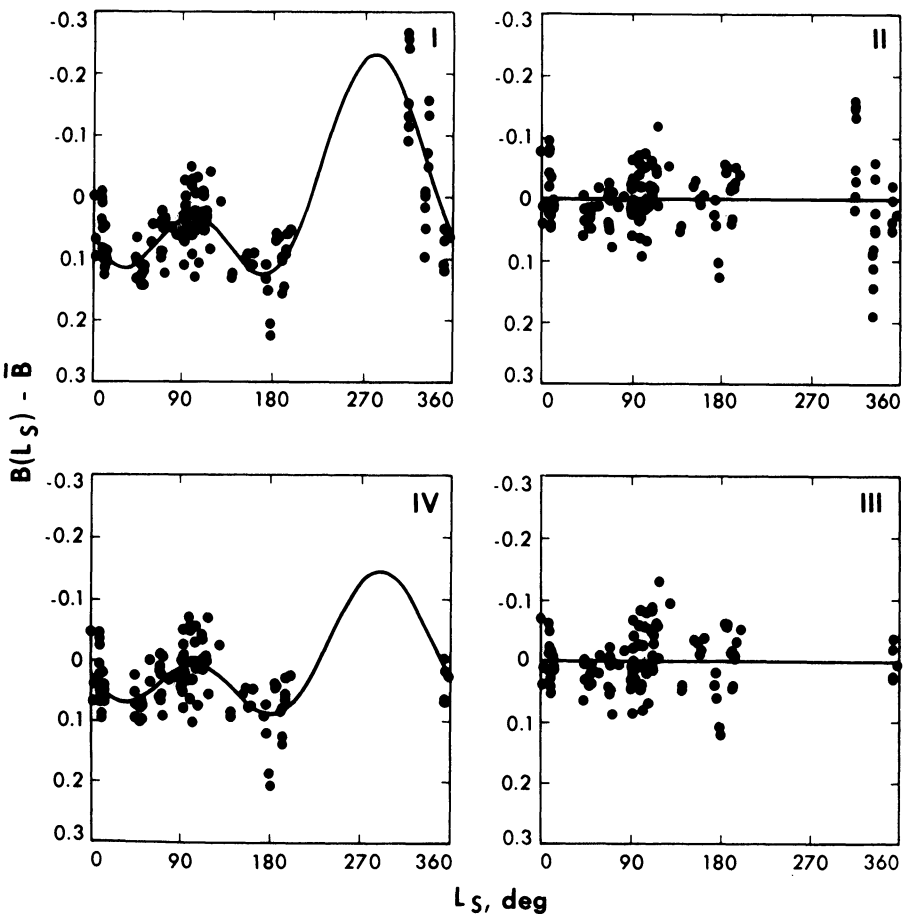

Fig. 13. Blue seasonal effect. (See Figure 6.)

https://doi.org/10.1017/S0074180900025493 Published online by Cambridge University Press

6.4. Observational errors and Martian variability

The striking differences between the rms residuals of different series of observations raise a number of questions. The first is whether the residual scatter represents observational errors or real fluctuations in the brightness of Mars.

The figures show that the scatter is not localized to a particular range of central meridian or phase angle. Aside from the 1958 data, the scatter does not appear concentrated to any range of L_S; since the scatter is quite small for the data at slightly larger L_S, a Martian seasonal effect seems unlikely. Furthermore, there is considerable overlap in L_S between series with markedly different scatter. Thus, one's initial impression is that the scatter is not Martian and must therefore be terrestrial.

We can go further and ask how much of the scatter *could* be due to Mars, by removing the estimated errors of observation. This is a fairly straight forward process for

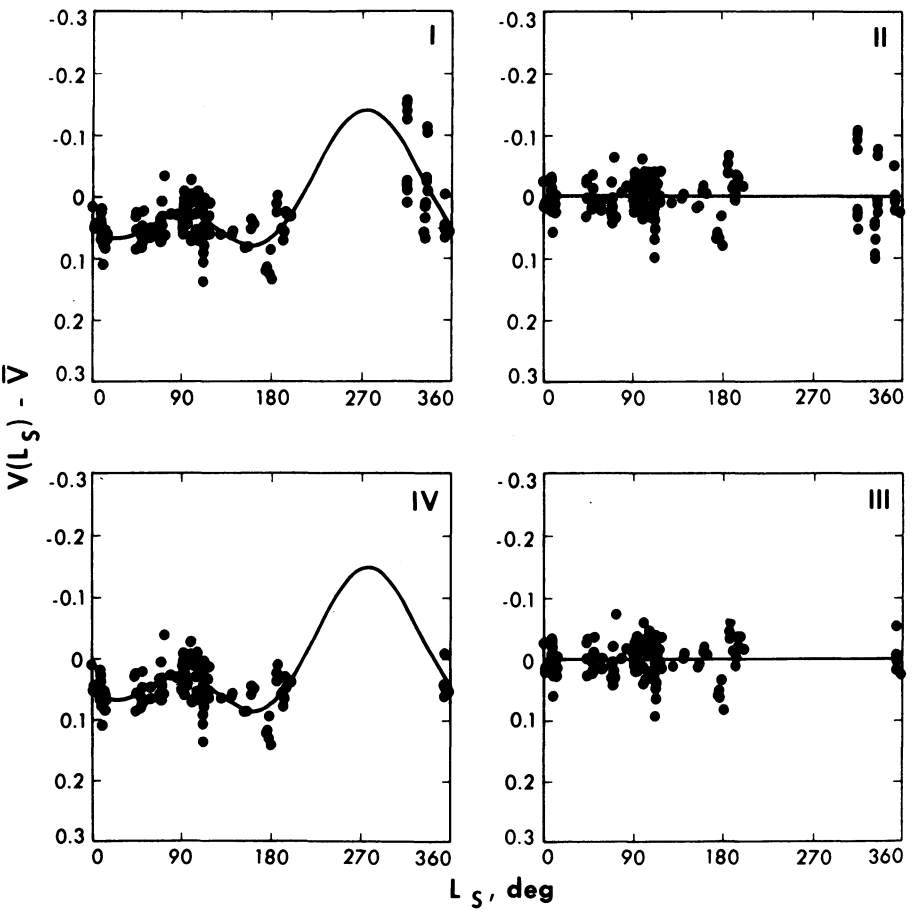

Fig. 14. Visual seasonal effect. (See Figure 6.)

https://doi.org/10.1017/S0074180900025493 Published online by Cambridge University Press

the later data, which have all been reduced with the same computer program. For these series we can estimate errors in two ways: from the internal scatter R of the extinction solution, and from the external scatter S of the fit to UBV standard stars. The latter method may give a more realistic assessment of night-to-night errors, but also includes the errors in the UBV standards, which are comparable to the Martian residuals. It is also complicated by the averaging of several observations for each star whereas the extinction residuals, like the residuals in the tables, refer to single observations. I therefore choose to use only the extinction residuals; this should lead to an upper limit for the intrinsic variability of Mars, because the random errors of transformation to the UBV system are not considered.

In writing the extinction program (Young and Irvine, 1967), I assumed that the observational error is proportional to air mass; the errors given are reduced to unit air mass. Although a steeper law is probably more accurate (Young, 1969), the errors at the mean air masses used can be correctly reproduced by using the relation assumed in the program. Thus, the rms error of observations is the product of the zenith error with the mean air mass of Mars.

My 1960 observations have a mean air mass of 1.452, so the expected rms errors are 0.028 in V, 0.029 in B, and 0.023 in U (see Table IV). The corresponding values for the 1961 observations (mean $\sec Z = 1.542$) are 0.009, 0.011, and 0.026. The mean-square observational errors for both sets combined (weighted according to the number of observations) are 0.000 50 in V, 0.000 59 in B, and 0.000 64 in U; the Martian variances from Table IX (Solution I) are 0.000 53, 0.002 12, and 0.005 03, respectively; so the possible Martian contributions are 0.000 03 in V, 0.001 53 in B, and 0.004 39 in U, corresponding to rms Martian variations of $\sigma_V = 0.005$, $\sigma_B = 0.039$, and $\sigma_U = 0.066$. (The value for σ_U is probably much too large, owing to the very approximate red-leak corrections.)

Similarly, one can estimate values from the Boyden and Le Houga data. As the exact air masses are not readily available, I have assumed the mean value (1.5) from the Agassiz Station data; this is probably an underestimate – especially for Boyden, because of the northern declination of Mars during these oppositions. For Le Houga, the expected rms observational errors in V, B, and U are 0.022, 0.026, and 0.032 respectively, which allow corresponding Martian variations of 0.000, 0.020, and 0.038 mag. For Boyden, the observational errors reduced to 1.5 air masses are 0.029, 0.031, and 0.032 which leave 0.033, 0.036, and 0.080 for Martian variations in V, B, and U. However, if a more realistic air mass of 2.0 is used, the observational errors rise to 0.019, 0.041, and 0.042, and the Martian variations become 0.021 mag. in V, 0.023 mag. in B, and 0.075 mag. in U; these figures agree better with the Agassiz Station and Le Houga results.

The low rms variation of the Le Houga data is particularly convincing, because they are the most numerous. Considering all three sets, and the exclusion of transformation errors, it seems safe to say that Mars actually varies randomly by no more than 0.01 in V, 0.02–0.03 in B, and 0.04 or so in U.

However, if we interpret the tabulated rms residuals as primarily due to observa-

tional errors, we have the remarkable conclusion that the best observations were made near sea level and the worst were made at the high-altitude observatories, which are generally regarded as having much better photometric conditions. In fact, both the Agassiz Station (except for U) and the Le Houga data compare favorably with best of the high-altitude data, which is all the more surprising because the former represent all-sky photometry, whereas the latter were made differentially.

The large errors in the Flagstaff magnitudes may be due in part to the large photomultiplier temperature variations that occur in Johnson's cold boxes if a heat-transfer liquid is not used (Young, 1963, 1966). Such liquids were used in the Le Houga and Boyden observations; the Agassiz Station data were taken at ambient temperature, a procedure which Stock has found to give very good results at Cerro Tololo. (The low quality of the Boyden data may be due to the difficulty of keeping trained observers at Boyden during the Harvard/NASA program.)

The Flagstaff *colors* are much better than the magnitudes, and generally better than the later colors, possibly because the Flagstaff B and U data were reduced as colors rather than magnitudes. Again, the low scatter of the Le Houga colors is surprising, as these data were reduced as magnitudes and differenced to obtain the colors.

The correlation of the residuals in adjacent bands can be estimated by comparing the rms residuals in the two magnitudes with the rms residual for the corresponding color. For example, the B and V residuals for 1958 are highly correlated, as the $(B-V)$ residuals are small; but the B and V residuals for Boyden are almost uncorrelated, as the $(B-V)$ residuals are larger than those in either magnitude alone. Such differences in correlation from one series to another are additional evidence that the residuals are largely observational error, because any Martian variations should be similarly correlated in all series.

7. Comparison with O'Leary

O'Leary (1967a, b) has also made UBV observations of Mars, at small phase angles near the 1967 opposition. His data can in principle be used to strengthen the determination of the phase effect at small phase angles, and to choose the most satisfactory of the Solutions I–IV discussed in the previous sections. Unfortunately his observations were all made differentially with respect to Spica, a close binary variable star with a most complex light curve; Shobbrock *et al.* (1969) have shown that one component is a β Canis Majoris star and the system is strongly affected by ellipticity effects. Thus Spica has variations, reflected in O'Leary's Mars data, both on a scale of a few hours and a few days, with a total variation of a tenth of a magnitude. These cannot be removed in detail because O'Leary does not give the individual observations. Finally, O'Leary's data were taken with non-standard filters and photomultiplier so that the transformation difficulties are certain to be more severe than those already discussed; indeed, O'Leary (1967a) says that his Kitt Peak data differ systematically from simultaneous Cerro Tololo observations by two tenths of a magnitude. At first sight it appears hopeless to salvage anything of value from these observations.

However, because O'Leary observed for several hours on each night, one can hope

that the β-Cephei-like variations of Spica have been partially averaged out in his tabulated nightly means. These can then be corrected for the known orbital variations of Spica, because O'Leary indicates the phase at which he observed.

As a preliminary check on his corrections for the Martian rotational effect, I have compared his mean rotational light curve (Figure 12 of his thesis) with the V light curves derived in Solutions I–IV (see Figure 15). The agreement is reasonably good; in view of the complications involved, no conclusion can be drawn from O'Leary's slightly smaller amplitude, which could be due to a Martian phase effect, a systematic transformation error (wrong effective wavelength), residual Spica variations, or other circumstances.

From O'Leary's (1967a) phase data and the visual light curve of Spica (Shobbrock *et al.*, 1969), I have determined approximate systematic corrections to O'Leary's nightly means. These are +0.018 mag. for April 14, 18, and 22; +0.07 for April 15 and 23; +0.010 for April 16, 20, and 24; and zero for April 13, 17, and 21. I have rejected the data for two cloudy nights (April 10 and 12). The corrections should probably be larger in B and U, but Shobbrock *et al.* do not give information for these colors. I have not corrected O'Leary's data for the seasonal effect, because they cover only 5° of L_S very close to the maximum at $L_S \approx 120°$; even in U, the variation over this range is less than a hundredth of a magnitude.

The corrected nightly means are plotted in Figures 16–18. Only Solutions I and IV are shown for comparison, because these include the seasonal effect. In V (Figure 18), the two agree equally well with O'Leary's data; in B (Figure 17) Solution IV agrees a little better, but the difference is small. In U (Figure 16), Solution I is clearly better than IV, which bends the wrong way at small phase angles; Solution I gives the larger

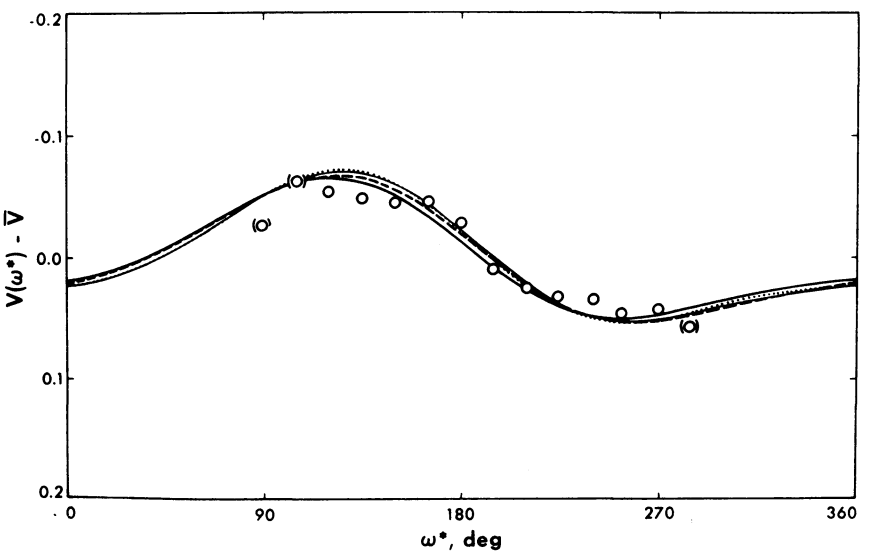

Fig. 15. Comparison of O'Leary's V light curve of Mars (circles) with the least-squares curves from Solutions I–IV. (Figure 8.)

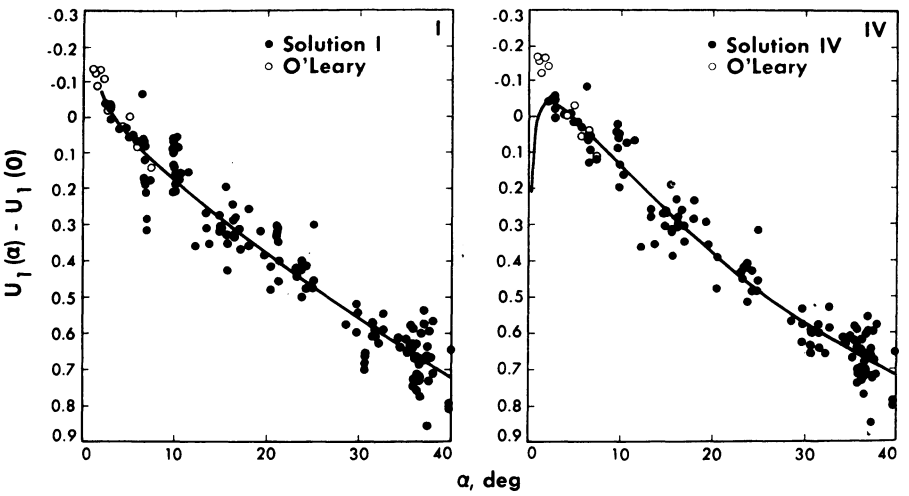

Fig. 16. Comparison of O'Leary's *U* phase data (open circles) with those for Solutions I and IV (curves and filled circles). Solution I fits the (corrected) O'Leary data quite well.

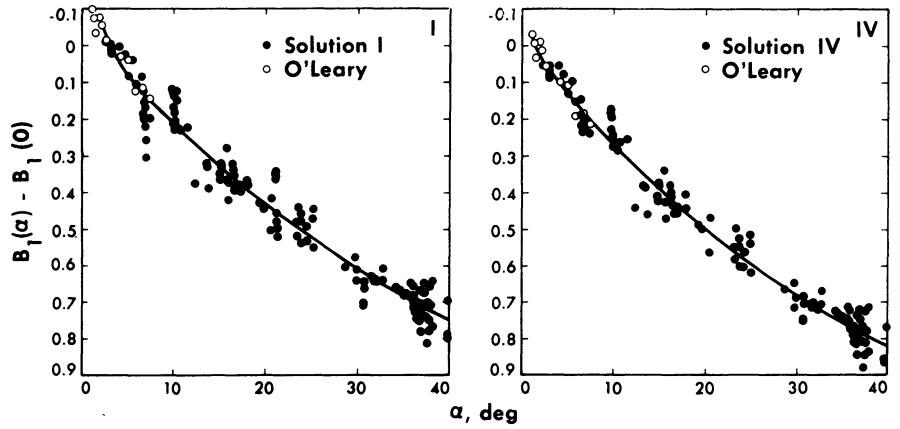

Fig. 17. Comparison of blue phase curves (see Figure 16). Here Solution IV fits O'Leary's data slightly better than Solution I, but the difference is small.

seasonal effect, so O'Leary's data give indirect support for the larger seasonal effect found by including the 1958 data (Solution I). I conclude that Solution I is probably closest to the truth.

The agreement of the extrapolation of this solution to small phase angles with O'Leary's data is quite unexpected. Thus the analytic interpolation formulae represent the data well even for phase angles as small as 2°. Because the least-squares solution is based on observations down to $\alpha = 3°$, the overlap with O'Leary's data (which extend to $\alpha = 7.5°$) is good, and there is no ambiguity in fitting the two together; this represents a substantial improvement over the fitting done by O'Leary on the basis of a *linear* extrapolation from larger phase angles.

https://doi.org/10.1017/S0074180900025493 Published online by Cambridge University Press

The smooth, continuous curvature of the phase curves, especially in B and U, disagrees with O'Leary's assertion of a *sudden* brightening at small (5–10°) phase angles. Indeed, if we regard the coefficient of the $1/\alpha$ term as representing the 'opposition effect', we see that it still amounts to a hundredth of a magnitude at $\alpha \approx 23°$. This also ignores the continued upward curvature of the phase relation at larger α, indicated by the negative α^2 terms. Thus, the name 'opposition effect' is misleading, and we should instead talk about the general *shape* of the phase curve.

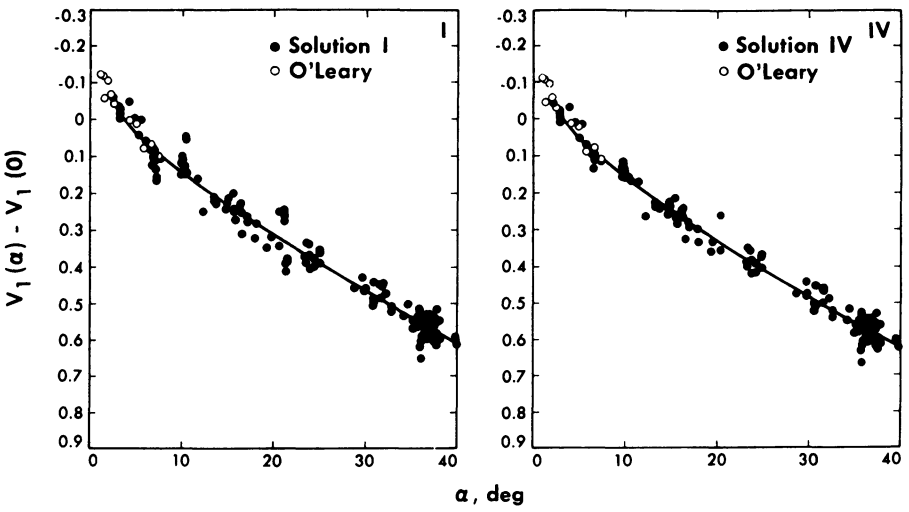

Fig. 18. Comparison of visual phase curves (see Figure 16). Solutions I and IV are similar, and both fit O'Leary's data well.

Furthermore, the present analysis does not support O'Leary's conclusion that the 'opposition effect' (interpreted as the $1/\alpha$ term) increases steadily from V to U. Indeed, this term is practically the same in all three colors. Differences would show most plainly in the $(B-V)$ and $(U-B)$ colors (Figure 19); although the *solutions* indicate a slightly greater effect in B than in V or U, the *data points* (including O'Leary's) do not indicate any opposition effect in the colors at all. In fact, although the $(B-V)$ color shows the well-known reddening with phase, the $(U-B)$ color is practically constant over the entire range of phase.

The phase curves for the colors are difficult to understand. Atmospheric scattering should be more important, relative to the surface, at short wavelengths and large phase angles. Thus one would expect Mars to become *bluer* at large phase – especially in $(U-B)$. Instead it becomes redder, but only in $(B-V)$. However, as the present data show that the marked wavelength dependence for the 'opposition effect' claimed by O'Leary does not exist, the various attempts to *explain* this fictitious phenomenon (O'Leary and Rea, 1968; Egan and Foreman, 1971; Mead, 1971) must be rejected. Furthermore, the phase independence of $(U-B)$ color (Figure 19b), together with the

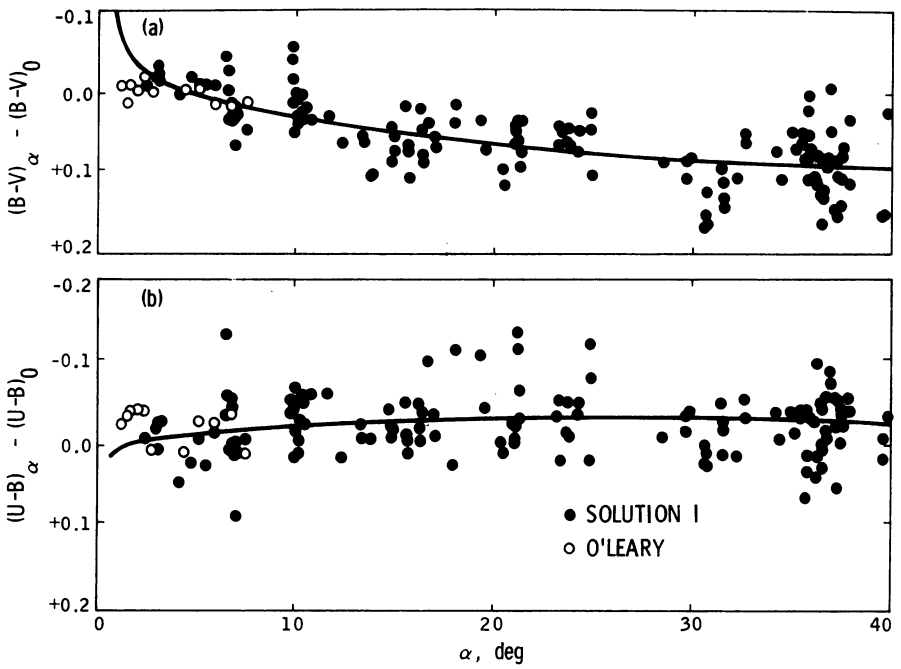

Fig. 19. (a) $(B-V)$ phase curve from Solution I, compared with O'Leary's data (open circles). (b) $(U-B)$ phase curve from Solution I, compared with O'Leary's data (open circles).

steep phase curves (Figure 16–18), suggests that, contrary to the claims of Ingersoll (1971), only a negligible fraction of the ultraviolet light received from Mars at large phase angles is due to Rayleigh scattering.

It is clear that a *realistic* interpretation of the Martian phase curves, allowing for the errors in the data, is still badly needed.

8. Conclusions

Let us adopt Solution I (Table IX) as the best. We see that the phase curves (Figure 16–18) are fairly well determined from 40° to about 2° phase angle. However, the extrapolation to zero phase is very uncertain. On the other hand, the mean rotation curves are very well determined; they change markedly with wavelength, as the $B-V$ and $U-B$ solutions show.

The seasonal effects and the absolute magnitudes and colors of the planet are very poorly determined. Even if we attribute the large scatter and zero-point terms of the 1958 data entirely to seasonal dust-storm effects, we are left with a wide range of zero-points: 0.05 in V, 0.05 in B, 0.16 in U, 0.07 in $(B-V)$, and 0.11 in $(U-B)$. These represent the uncertainties due to systematic differences between different UBV photometers.

https://doi.org/10.1017/S0074180900025493 Published online by Cambridge University Press

These uncertainties are inherent in the UBV 'system', which is poorly defined for objects like Mars. Thus the fundamental ambiguities of this photometric system prevent us from ever giving the brightness (or albedo) of Mars to an accuracy better than 0.05 mag.

These systematic errors are much larger than the random fluctuations of the planet's brightness, at least outside of the dusty season near $L_S \approx 270°$. Thus, although additional long, homogeneous series of UBV data would improve our knowledge of seasonal (and, to some extent, phase) effects, the albedo problem requires an entirely new approach. To determine the albedo of Mars accurately, we would need a long series of observations in a well-defined photometric system; the means of setting up such a system are described elsewhere (Young, 1973).

The large size of the seasonal effect shows that a very lengthy observational program (several years) would be required. As all existing data suffer from the same systematic-error problem, it may not be practical to combine *any* of them with new, error-free data.

Finally, one must consider the consequences of such systematic errors in other planetary albedoes. If one allows for the additional uncertainties in the magnitudes and colors of the Sun, one must conclude that any planetary albedo may be uncertain by at least ten percent, apart from the effect of errors in size. For dark objects like Mars, Moon, and Mercury, the albedo error has a small effect on the planetary heat budget, as a fractional albedo error of $(\Delta A/A) = f$ is only an error of $[fA/(1-A)]$ in absorbed energy. Thus if $A = 0.2$, an error f of 10% is only a 2.5% error in absorbed radiation. But for a bright planet like Venus, with $A \approx 0.8$, $f = 0.1$ corresponds to a 40% error in the calculated heat budget. Better data are certainly needed.

Acknowledgements

This paper presents the results of one phase of research carried out at the Jet Propulsion Laboratory, California Institute of Technology, under Contract No. NAS 7-100, sponsored by the National Aeronautics and Space Administration.

References

Cousins, A. W. J. and Stoy, R. H.: 1963, *Roy. Obs. Bull.*, No. 64.
De Vaucouleurs, G.: 1960, *Planetary Space Sci.* **2**, 26.
Egan, W. G. and Foreman, K. M.: 1971, in C. Sagan, T. C. Owen, and H. J. Smith (eds.), 'Planetary Atmospheres', *IAU Symp.* **40**, 156.
Fernie, J. D. and Watt, V.: 1967, *Astrophys. J.* **150**, L113.
Guthnick, P. and Prager, R.: 1914, *Veröff. Kgl. Sternw. Berlin-Babelsberg* **1**, 1.
Ingersoll, A. P.: 1971, in C. Sagan, T. C. Owen, and H. J. Smith (eds.), 'Planetary Atmospheres', *IAU Symp.* **40**, 170.
Irvine, W. M., Simon, T., Menzel, D. H., Charon, J., Lecomte, G., Griboval, P., and Young, A. T.: 1968a, *Astron. J.* **73**, 251.
Irvine, W. M., Simon, T., Menzel, D. H., Pikoos, C., and Young, A. T.: 1968b, *Astron. J.* **73**, 807.
Johnson, H. L. and Gardiner, A. J.: 1955, *Publ. Astron. Soc. Pacific* **67**, 74.

Johnson, H. L., Mitchell, R. I., Iriarte, B., and Wisniewski, W. Z.: 1966, *Comm. Lunar Planet. Lab.* **4**, No. 63.
Lawrence, L. C. and Reddish, V. C.: 1965, *Publ. Roy. Obs. Edinburgh* **3**, No. 9, 280.
Mead, J. M.: 1971, in C. Sagan, T. C. Owen, and H. J. Smith (eds.), 'Planetary Atmospheres', *IAU Symp.* **40**, 166.
Meiller, V.: 1964, *U.S. Naval Obs. Circ.*, No. 98, 1964.
O'Leary, B. T.: 1967a, Technical Report on NASA Grant NsG 101-61, Space Sciences Laboratory Series 8, Issue 103 (Ph.D. thesis, Astronomy Department, University of Calif., Berkeley).
O'Leary, B. T.: 1967b, *Astrophys. J. Letters* **149**, L147.
O'Leary, B. T. and Rea, D. G.: 1968, *Icarus* **9**, 405.
Schmidt-Kaler, T.: 1961, *Observatory* **81**, 246.
Shao, C. Y., and Young, A. T.: 1965, *Astron. J.* **70**, 726.
Shobbrock, R. R., Herbison-Evans, D., Johnston, I. D., and Lomb, N. R.: 1969, *Monthly Notices Roy. Astron. Soc.* **145**, 131.
Young, A. T.: 1957, *Publ. Astron. Soc. Pacific* **69**, 568.
Young, A. T.: 1963, *Appl. Opt.* **2**, 51.
Young, A. T.: 1966, *Observatory* **86**, 71.
Young, A. T. and Irvine, W. M.: 1967, *Astron. J.* **72**, 945.
Young, A. T.: 1969, *Appl. Opt.* **8**, 869.
Young, A. T. and Collins, S. A.: 1971, *J. Geophys. Res.* **76**, 432.
Young, A. T.: 1973, in *Methods of Experimental Physics*, Academic Press, New York, Vol. 12A, Chapter 3.